Geo.Alp, Vol. 13 2013 141 - 182

Field trip 4

Deep water sedimentation on top of a growing orogenic wedge - interaction of thrusting, erosion and deposition in the Cretaceous Northern Calcareous Alps

Hugo Ortner

Institute of Geology, University of Innsbruck, Innrain 52, 6020 Innsbruck

1 Goals and highlights of excursion

This field trip will show deformation and related deposition during stacking of thrust sheets in the Cretaceous Northern Calcareous Alps. The itinerary of the field trip is chosen to illustrate different types of synorogenic sediments following the definition of Ortner (2003a) and Ortner & Gaupp (2007): The **first part** of the field trip will visit the spectacular outcrops at Krabachjoch in the Arlberg region, where a klippe of the Inntal thrust sheet overlies the synorogenic deposits of the Lech Formation. The latter is an example of **upper-footwall deposits** in the foreland of a thrust sheet. The **second part** of the field trip visits the Gosau Group of Muttekopf in the vicinity of Hanauer Hütte. There, coarse clastic continental to deep marine synorogenic sediments overlie the deeply eroded Inntal thrust sheet. This type of synorogenic succession has been termed **thrust-sheet-top deposits**. Up to 1000 m of mostly coarse clastic, deep marine deposits are preserved in a km-scale syncline. Several angular unconformities document fold growth during deposition; the most prominent angular unconformity in the area is the Schlenkerkar unconformity that formed as a consequence of folding and concurrent tear faulting, and was recently defined as the type example of a fault-related progressive unconformity (Ortner et al., 2015). The vicinity of the Hanauer Hütte offers seismic scale outcrops of synorogenic sediments and their relationship to preorogenic deposits comparable to the Southern Pyrenees (e.g., Puigdefabegras et al., 1992).

The distribution of Cretaceous upper-footwall- and thrust-sheet-top deposits in the western Northern Calcareous Alps allows to separate initial Cretaceous nappe-stacking from later thrust sheet movements, and in-sequence from out-of sequence thrusting. The analysis of the distribution of different types of synorogenic deposits shows that the Inntal thrust is out-of-sequence (Ortner, 2003a), and splays from the Lechtal thrust. In the Karwendel mountains, the Inntal thrust looses offset, the continuity of Inntal- and Lechtal thrust sheet is partly preserved (e.g., Figs. 48 and 96 in Ampferer, 1942; Ortner & Kilian, 2013).

2 Geological setting and introduction of basic concepts

The Northern Calcareous Alps formed in a two-stage process (Froitzheim et al., 1996; Neubauer et al., 2000; Schmid et al., 2004). In the western part of the Northern Calcareous Alps, initial inversion of the former passive continental margin occurred during the late Early to Late Cretaceous in the foreland of the closure of the Meliata part of the Neotethys ocean (Fig. 1a; Frank, 1987; Ortner, 2003a). At the same time, subduction of the Alpine Tethys, also referred to as Penninic ocean, had already started. Thus, the Adriatic microplate and the Northern Calcareous Alps at its northwestern edge either occupied an intermediate position between two subductions in the Upper Cretaceous (e.g., Schmid et al., 2004; Wagreich, 2001), or

the position of a single subduction shifted in time (Stüwe & Schuster, 2010). At the time of stacking of thrust sheets, the Northern Calcareous Alps were a typical foreland fold-and-thrust belt. In a second stage, the Northern Calcareous Alps were transported piggy-back as a part of the upper plate onto the European lower plate (Fig. 1b). This process culminated in continental collision during the Eocene that extincted the Penninic ocean. From a structural point of view, Cretaceous nappe stacking and subsequent transport onto Penninic units are separate events in terms of transport directions: Cretaceous nappe stacking and folding was NW-directed, while Paleogene shortening was N to NNE-directed (Eisbacher & Brandner, 1996). WNW-striking fold axes are well developed in the thrust sheets of the Rhenodanubian Flysch (Rothmund, 2015) and the Arosa Zone (Biehler, 1990). However, post-collisional Paleogene and Neogene shortening repeated the structural history with Late Paleogene NW-transport, followed by Neogene NNE-directed shortening (Ortner, 2003b; Peresson & Decker, 1997).

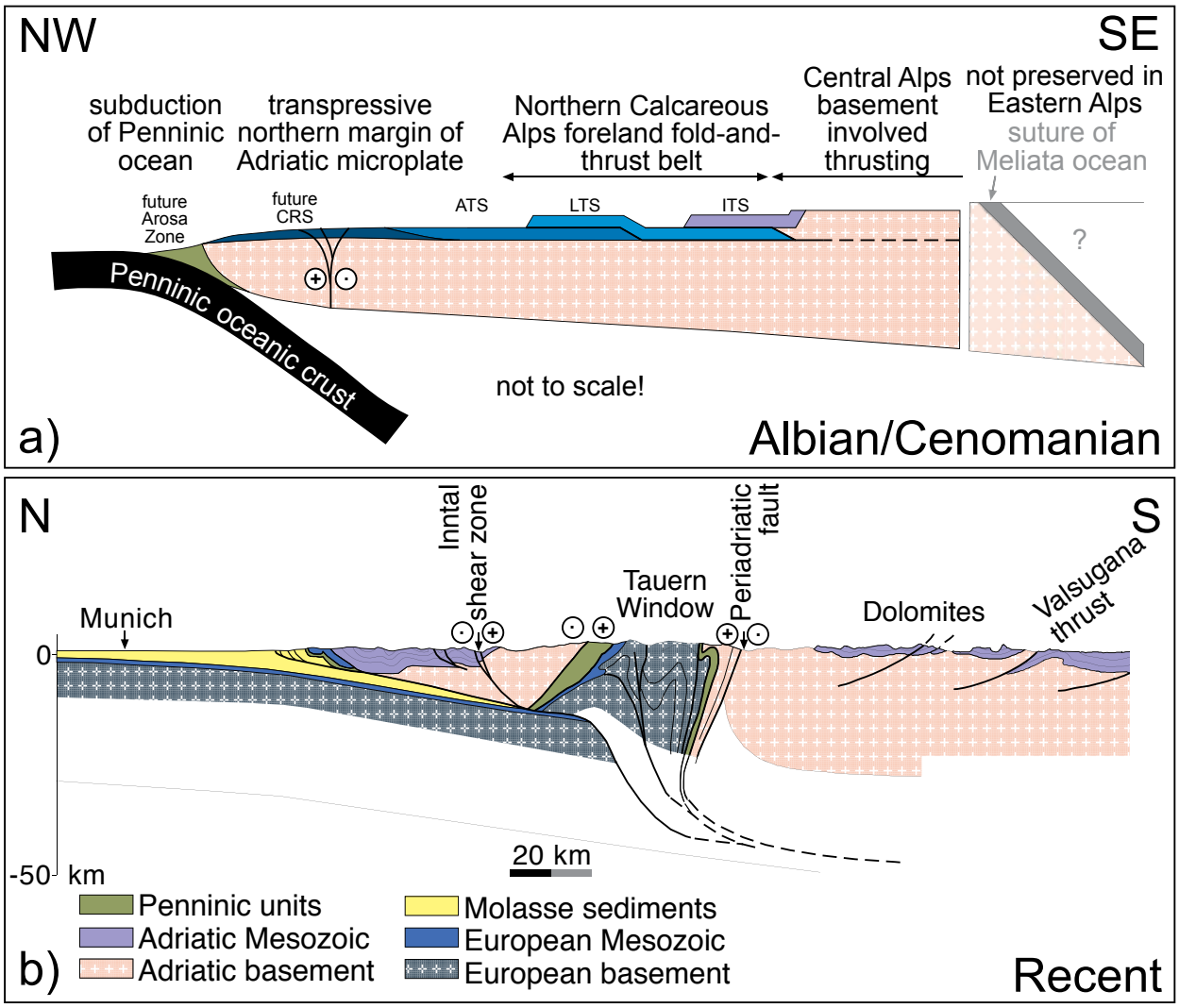

Fig. 1: The two-stage evolution of the Northern Calcareous Alps. (a) Stacking of thrust sheets at the boundary from the Early to the Late Cretaceous. The foreland fold-and-thrust belt of the Northern Calcareous Alps developed in the foreland of the closure of the Meliata ocean. Penninic subduction had, however, already started (adapted from Wagreich, 2001). CRS = Cenomanrandschuppe, ATS = Allgäu thrust sheet, LTS = Lechtal thrust sheet, ITS = Inntal thrust sheet. (b) Present day cross section of the Eastern Alps east of Innsbruck. The Northern Calcareous Alps are transported piggy-back on the Helvetic and Penninic thrust sheets, that form the fold-and-thrust belt related to Cenozoic orogeny, onto the European plate (adapted from Lammerer & Weger, 1998). Legend denotes paleogeographic affinity of units.

The thrust sheets of the Northern Calcarous Alps were essentially defined at the start of the 20th century by Ampferer & Hammer (1911) in the west, and, for the central part in Salzburg and Upper Austria, by Hahn (1912, 1913). The two tectonic classifications are, with some modifications (e.g., Frisch & Gawlick, 2003; Tollmann, 1976), still in use. In the western Northern Calcareous Alps, three main thrust sheets are present. These are, from base to top, the Allgäu thrust sheet, the Lechtal thrust sheet and the Inntal thrust sheet (Fig. 2c). At the northern margin of the Allgäu thrust

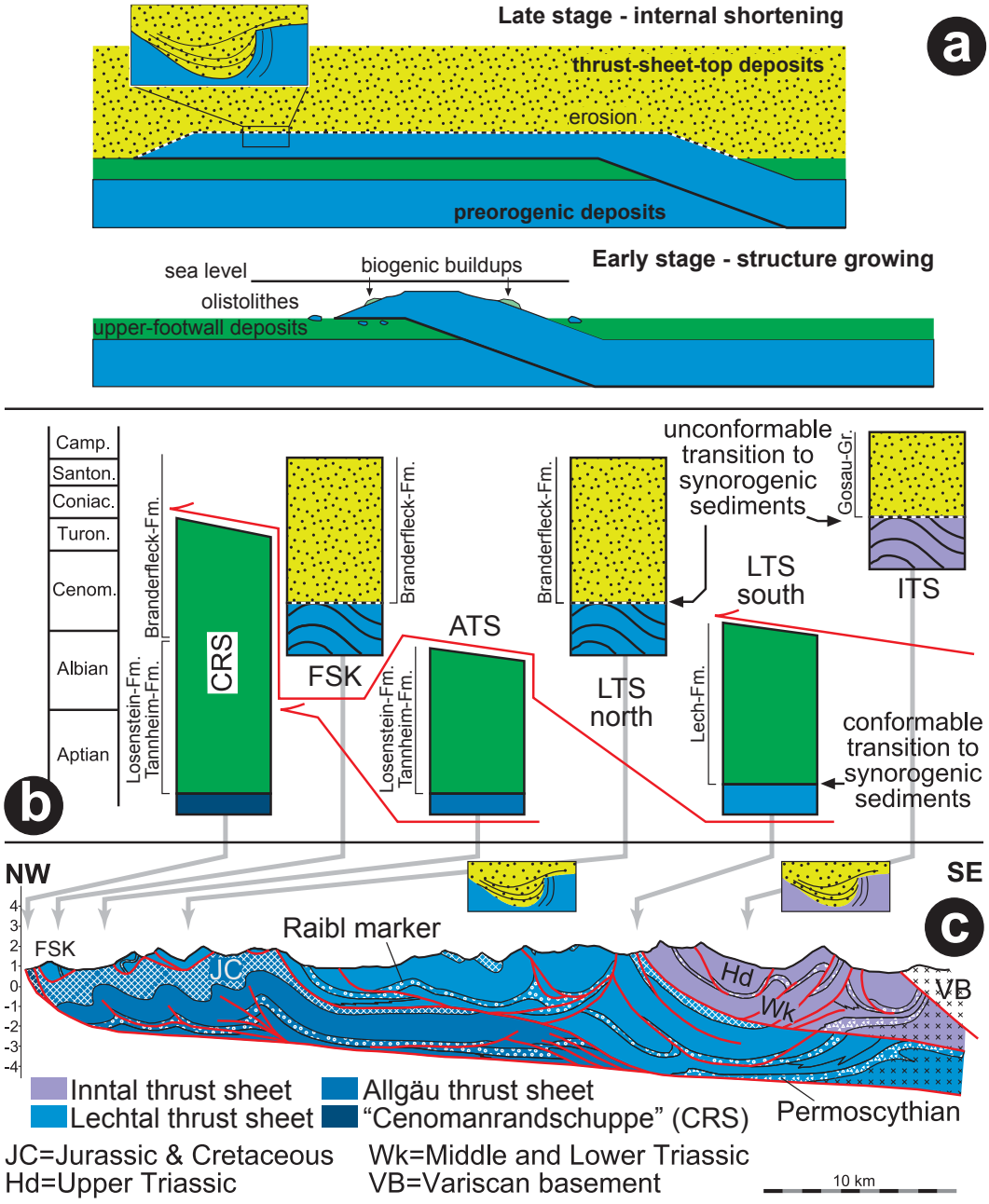

Fig. 2: Relationship of thrusting to synorogenic sedimentation. (a) Ramp-flat model illustrating the effects of thrusting in a deep marine environment during an early stage (bottom) and a late stage (top). (b) Distribution and timing of synorogenic sedimentation in the Northern Calcareous Alps roughly along the trace of the cross section below. (c) Cross section of the Northern Calcareous Alps (adapted from Eisbacher et al., 1990). Trace of section given in Figure 3. CRS = Cenomanrandschuppe, FSK = Falkenstein klippe, ATS = Allgäu thrust sheet, LTS = Lechtal thrust sheet, ITS = Inntal thrust sheet.

sheet, a tectonically deeper unit, the *Cenoman-randschuppe* (a marginal slice characterized by Cenomanian sediments) is present; the Inntal thrust sheet carries the klippen of the Krabach-joch nappe in a few places.

The thrust distance of the nappes is large. Eisbacher et al. (1990) reconstructed some 20 km for the Inntal thrust, which is the thrust plane at the base of the Inntal thrust sheet. The definition of the large thrust sheets is based on the observation of old rocks thrust onto much younger, usually Cretaceous rocks (Fig. 3). However, in map view, most of the large thrusts of the Northern Calcareous Alps end laterally, where the stratigraphic offset disappears. The Lechtal thrust, for example, ends near Lech in the Arlberg region (Fig. 3, north of label 1; e.g., Spengler, 1953), and is replaced by the Mohnenfluh thrust to the west. This suggests that the thrusts grew laterally, before individual, initially separated segments joined to form a throughgoing thrust (e.g., Mazzoli et al., 2005 for the Apennines). Thrusting in the Northern Calcareous Alps took place in a transpressive setting (Linzer et al., 1995; Wagreich, 2001), and the thrust sheets are dissected by numerous subvertical NW-striking tear faults that terminate against the thrust plane at the base of the thrust sheet (Eisbacher & Brandner, 1996).

Initial thrust activity is monitored by synorogenic sediments. Synorogenic sediments are deposits that are influenced by tectonic processes during mountain building. They can be exported from the area of active structural growth. Siliziclastic material deduced from exhumation in internal parts of an orogen will reach the foreland of the thrust belt and represents the sedimentary signal of mountain building, especially in carbonate-dominated continental margins. The onset of thrusting in the Late Cretaceous of the Northern Calcareous Alps is associated with a change from deposition of pelagic, often condensed limestones formed from coccolithe ooze (Flügel & Fenninger, 1966; Garrison & Fischer, 1969) to marls intercalated with sandstones. The processes in the zone of shortening can be described using a ramp-flat model (Fig. 2a; Ortner, 2003a; Ortner & Gaupp, 2007). Incipient thrusting will lead to the creation of submarine topography, and slabs of rock may break off the allochthon creating olistoliths that are overthrust subsequently. While offset across the thrust increases and the thrust sheet climbs up the ramp, relative sea level falls above the growing hanging-wall anticline, until conditions are suitable for the growth of small, shortlived carbonate platforms or biogenic buildups. If eroded, this material is redeposited into the surrounding basins. Upon further growth, the hanging-wall anticline is uplifted above sea level. It is eroded and the thickness of the thrust sheet reduced. As a consequence, the thrust sheet is mechanically weaker and gets deformed internally. This is expressed by folding during further shortening, while continental sedimentation starts.

In respect to a thrust sheet two types of synorogenic deposits can be distinguished (Fig. 2a, b; Ortner, 2003a): (1) **upper-footwall deposits** are found in the foreland of a thrust that becomes the upper footwall as the thrust propagates. These sediments are characterized by a conformal transition from passive-margin to synorogenic sediments, the occurrence of olistolithes derived from the thrust sheet, and the local occurrence of shallow water detritus derived from short-lived biogenic buildups. As these sediments are deposited as a thrust sheet approaches the point of observation, deposition coarsens to the top. (2) **thrust-sheet-top deposits** are found on top of the large scale hanging-wall anticline. They overlie an erosion surface that forms during exhumation and shortening, and therefore this erosion surface is developed as an angular unconformity. Progressive shortening during deposition is expressed by the formation of numerous angular unconformities within the thrust-sheet-top deposits, which are growth strata.

The nomenclature of growth strata is not well established in the Alpine literature, and therefore I give an introduction here. Growth strata are sediments that are deposited on growing folds or faults, and record incremental strain as the structures are buried. The stratal geometries developed depend on the relationship between the rate of deposition R_a and the vertical growth of a structure R_u (Fig. 4a; Ford et al., 1997; Riba, 1976). When $R_a < R_u$, the point of onlap of wedge-shaped

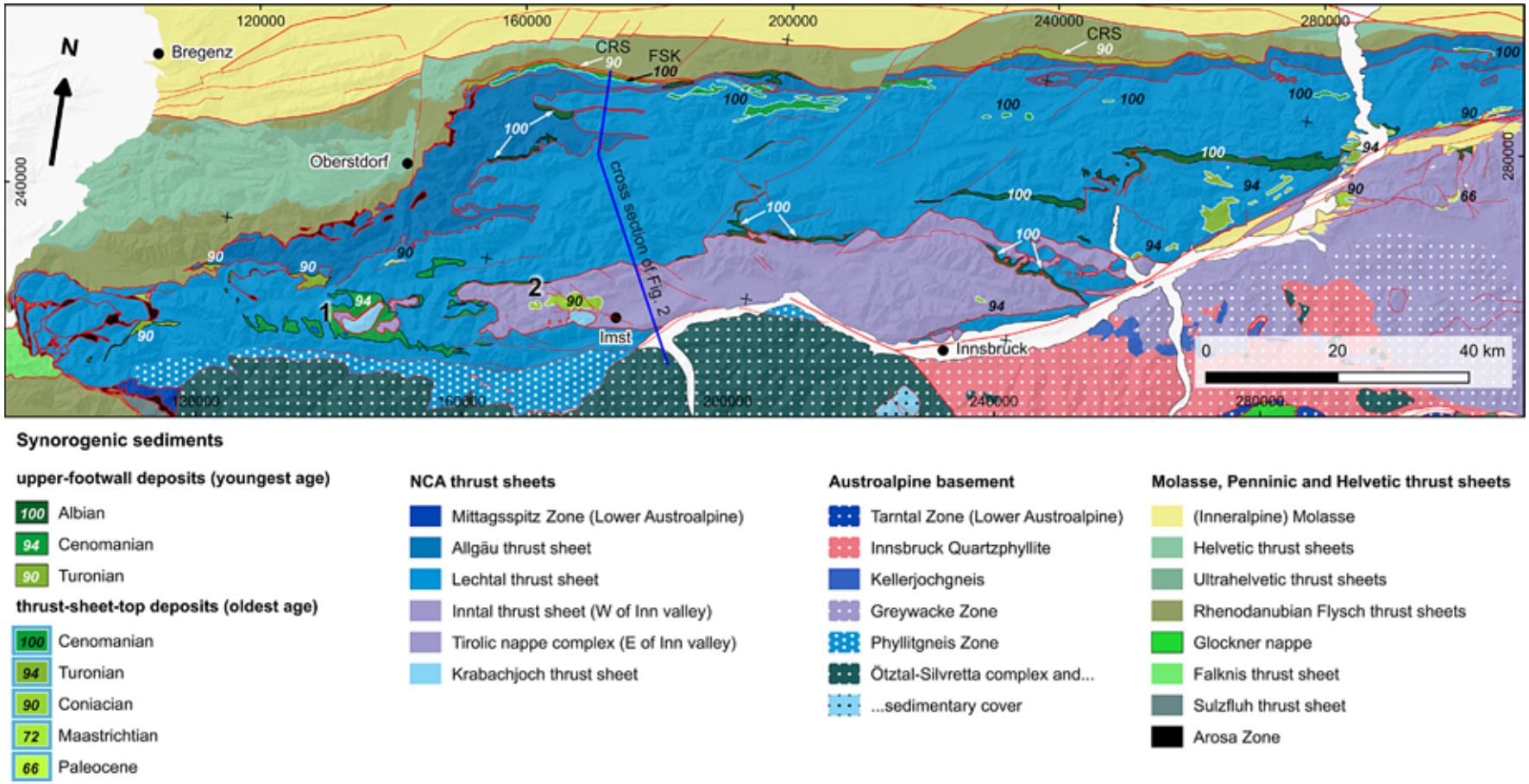

Fig. 3: Tectonic map of the western part of the Northern Calcareous Alps. Tectonic subdivision according to Tollmann (1976). Synorogenic sediments subdivided into upper-footwall- and thrust-sheet-top deposits. For the first, the youngest age below the thrust of the overlying tectonic unit is given, for the latter the age of the oldest sediments above the erosional unconformity. 1 = Flexenpass and Zürs, day 1 of the field trip, 2 = western part of Gosau Group of Muttekopf near Hanauer Hütte, day 2 and 3 of the field trip. Abbreviations: CRS = Cenomanrandschuppe, color denotes upper-footwall deposits reaching into the Turonian. FSK = Falkenstein klippe, an external part of the Lechtal thrust sheet. Graticule: MGI/Austria GK M28 (EPSG: 31257).

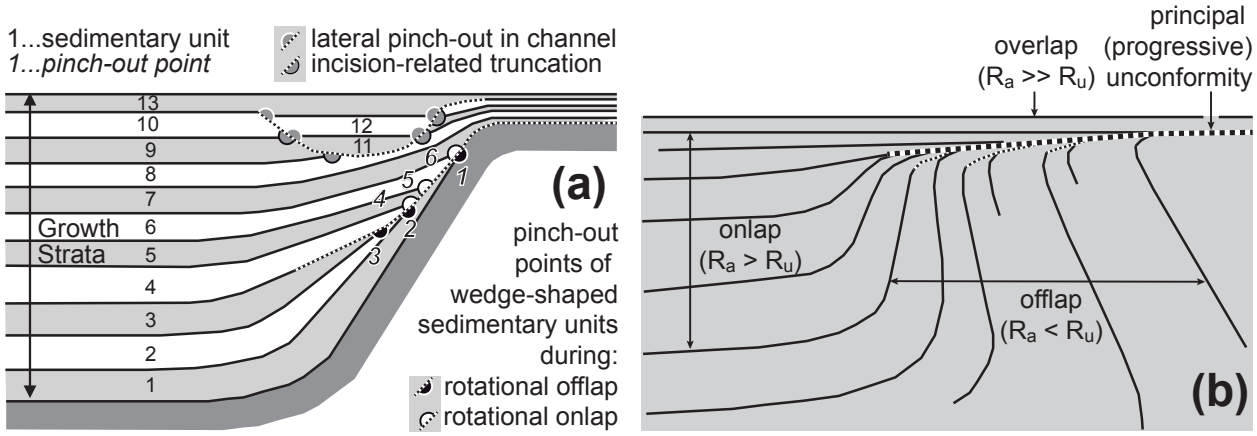

Fig. 4: Nomenclature of angular unconformities in growth strata on growing folds (modified from Ortner et al., 2015). a) Shift of pinch-out-points of sedimentary units onlapping a growing fold. 1-13 = successive stratigraphic units in growth strata sequence, *1-6* = pinch out points of stratigraphic units 1-6. Note pinch-out points *1-3* shifting away from the crest of the fold during rotational offlap, and pinch-out points *4-6* moving toward the crest of the fold during rotational onlap. Overlapping units (e.g., bed 13) do not have pinch-outs. Incision events may cause angular unconformities if the channel is in a zone of structural growth, as shown by the lateral pinch-out on the right side of the channel of beds 11 and 12. The left side of this channel is outside of the zone of structural growth, and no angular unconformity is developed. b) Development of a progressive angular unconformity during the growth of an anticline-syncline pair with fixed limb length. When the rate of deposition R_a is kept constant, rapid initial vertical growth of the fold will cause rotational offlap. As vertical growth decelerates in the later stages of fold development, the relative rate of deposition increases, and rotational onlap, eventually followed by overlap will develop.

sedimentary units will move away from the structure, and rotational offlap develops. If $R_a > R_u$, the point of onlap moves toward and climbs up the structure, creating rotational onlap. Rotational overlap is observed when $R_a >> R_u$, the structure is buried. Growth histories of folds documented by syntectonic sediments are typically characterized by fixed limb length folding and a constant rate of shortening that leads to rapid initial vertical growth that slows down when the fold gets tighter before the fold locks (Fig. 4b; e.g., Ortner et al., 2015). If the rate of deposition of syntectonic sediments is constant, initial rotational offlap will be followed by rotational onlap and finally rotational overlap. In such a case, all individual angular unconformities will merge toward the crest of the growing fold to form the principal progressive unconformity (Riba, 1976). However, many angular unconformities are not related to rotational offlap or onlap, but to erosion and subsequent infill (Fig. 4a; Ford et al., 1997).

3 Excursion Route and Stops

The field trip intends to demonstrate the two different types of synorogenic sediments that were described above. The first part of the field trip in the vicinity of Zürs in the Arlberg region will showcase upper-footwall deposits (day 1; 1 of Fig. 3) as developed on the Zürs swell of the Lechtal thrust sheet, below the Inntal thrust. The second part will show thrust-sheet-top sediments in the vicinity of the Hanau Alpine hut (day 2-3; 2 of Fig. 3).

3.1 Upper footwall-deposits in the vicinity of the Krabachjoch

3.1.1 Local geology

The Krabachjoch was one of the first areas in which a thrust sheet was recognized in the Northern Calcareous Alps (Richthofen, 1859). In fact,

Fig. 5: Geologic map of the western part of the Krabachjoch klippen, compiled from Ampferer et al. (1932), Doert & Helmcke (1976), Moser & Pavlik (2011) and May (1998). Numbers 1 - 5 denote field trip stops. Diagram shows fold axes (fa) of the Paleogene Erli syncline and the Neogene Kugla syncline. Graticule: MGI/Austria GK West (EPSG: 31254).

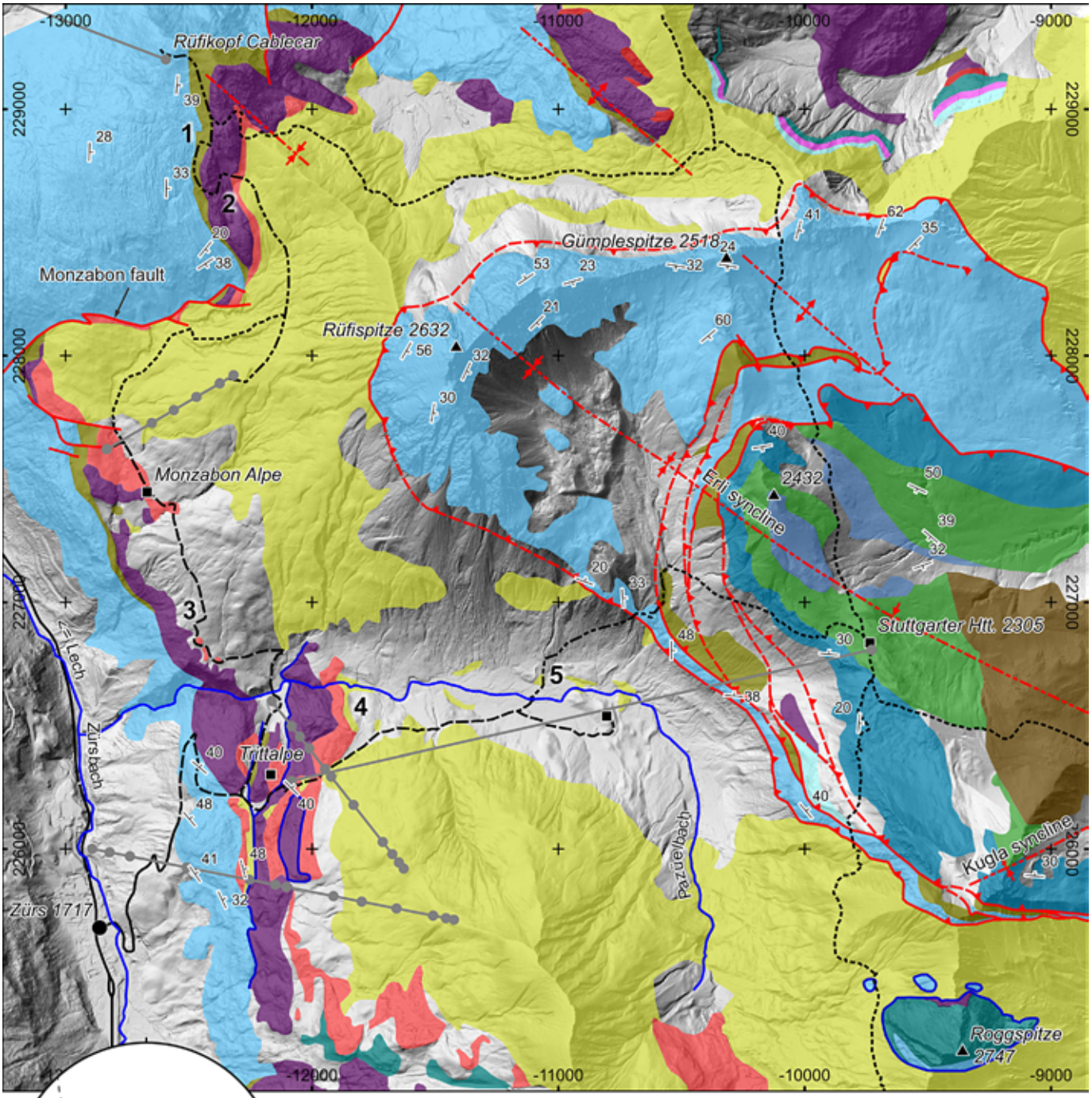

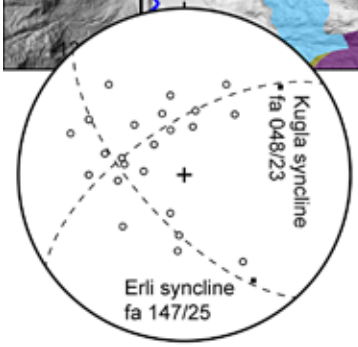

Important places

- Summit
- Populated place
- Alpine hut
- lift post

Formations

- Lech Fm.
- condensed Jurassic/Cretaceous of Zürs swell
- Ammergau Fm.
- Allgäu Fm.
- Oberrhät limestone
- Kössen Fm.
- Hauptdolomit
- Raibl beds
- Arlberg beds
- Partnach beds
- Alpine Muschelkalk Group

Tectonic symbols

- Trace of axial plane (anticline/syncline)
- fault
- fault, suspected
- glide plane, olistolith boundary

Road and path network

- path
- small dirtroad
- dirtroad
- road
- chairlift
- creek

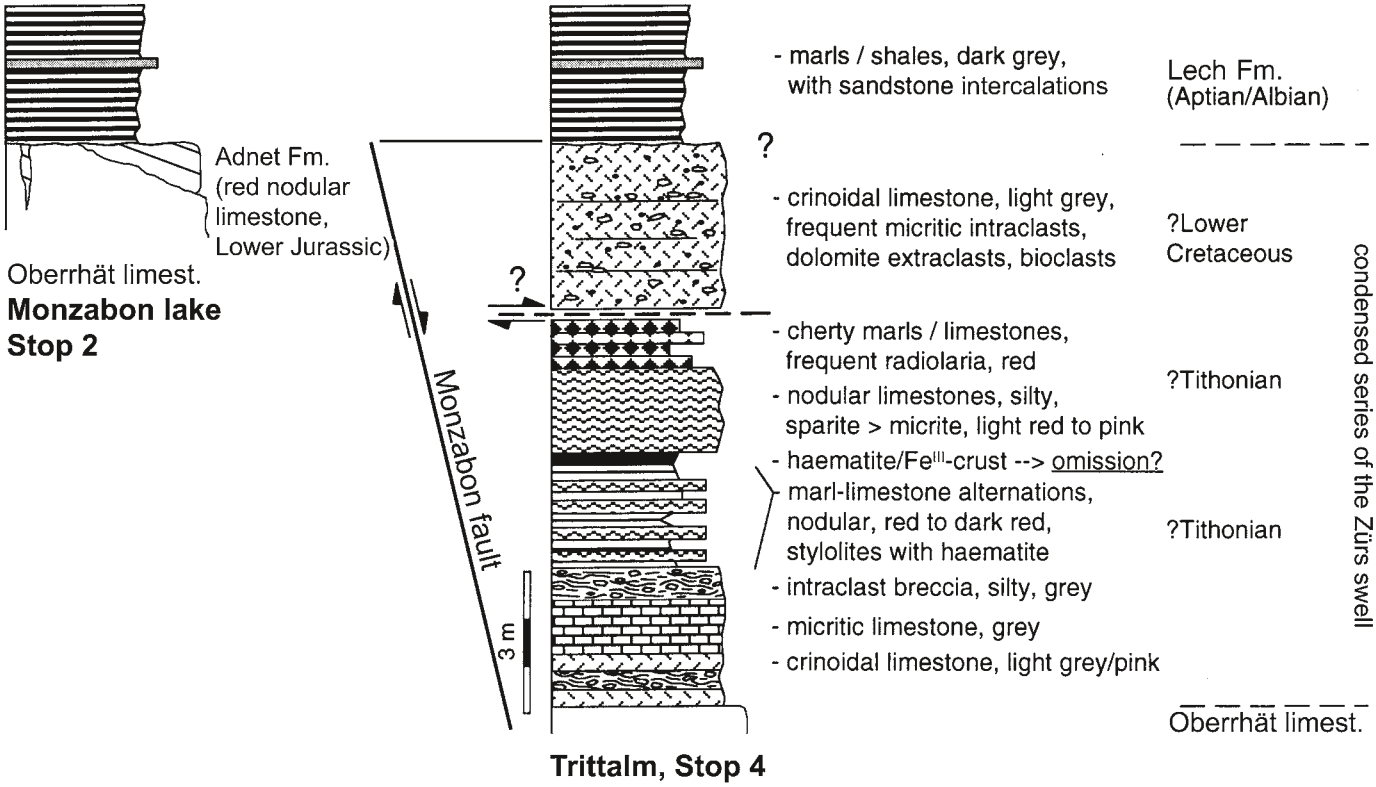

Fig. 6: Sedimentary succession on the Zürs swell in the vicinity of the Monzabon fault (adapted from Gaupp et al., 1997).

the Krabachjoch klippen are one of the most impressive outcrops of thrust sheets and their boundaries. Three thrust sheets are present: The Lechtal thrust sheet is the lowermost unit, overlain by the Lower Krabach klippe, which is part of the Inntal thrust sheet, and the Upper Krabach klippe belonging to the Krabachjoch thrust sheet (Fig. 3). All units are found in the core of a structural basin formed by the overprinting of the NE-trending Kugla syncline and the NW-trending Erli syncline (Fig. 5; May & Eisbacher, 1999).

The sedimentary succession exposed in the **Lechtal thrust sheet** reaches from the Norian Hauptdolomit to the Lech Fm., which reaches into the Cenomanian, but ends in the Albian in the field trip area (Eynatten, 1996; Huckriede, 1958). Most units have a reduced thickness, especially the Jurassic to Lower Cretaceous units. Jacobshagen (1965) termed this zone the *Zürser Schwelle* (Zürs swell), a Jurassic-Cretaceous deep swell characterized by very small rates of deposition and condensation. The few meters of sediment on the Zürs swell contrast with more than 1000 m of basinal sediments in the northerly adjacent region (Jacobshagen, 1965). The main reason for this contrast in thickness is Liassic rifting at the northwestern margin of the Adriatic plate in the course of the opening of the Penninic ocean (e.g., Froitzheim & Manatschal, 1996). Thickness differences in post-rift sediments of Upper Jurassic and Lower Cretacous age essentially mimic those of the syn-rift sediments, however, local Jurassic to Cretaceous faulting causes thickness contrasts within sediments of this age (Fig. 6).

A good example of a paleofault active during the Jurassic and Cretaceous is the E-W-striking Monzabon fault (Fig. 5) that offsets all lithologic boundaries and disappears within the Lech Fm. As remnants of the condensed series of the Zürs swell are found along the fault, and since the Lech Fm. is in direct contact with the fault, the main activity of the fault was probably during deposition of the Lech Fm. Fault activity was probably accompanied by block tilting and associated

gliding along bedding planes. The distribution of the Oberrhät limestone and Kössen Fm. north of and near the eastern tip of the fault suggests that both units moved toward the fault with the Kössen Fm. as a detachment. Part of the moving units were cut off by the Monzabon fault and progressively moved down the fault. Also the block south of the Monzabon fault shows evidence of gliding. In the vicinity of the Trittalpe (Fig. 5), the succession from the Oberrhät limestone to the condensed series of the Zürs swell is repeated four times, and one of the glide planes clearly climbs upsection to the north. Gliding was active during the onset of deposition of the Lech Fm., as the Lech Fm. underlies some of the glide blocks.

The Lech Fm. consists of shales, with a few intercalations of turbiditic sandstones. The upper part of the Lech Fm. contains another set of olistolithes (May & Eisbacher, 1999). The most prominent of these olistolithes is the Roggspitze (SE corner of Fig. 5). It is mainly built of the Lower Jurassic deep-water limestones of the Allgäu Fm. The Allgäu Fm. contains blocks of Hauptdolomit and Oberrhät limestone, which are not in a systematic sedimentary succession and are reminiscent of the central Lechtal Alps where it contains olistolithes (Bischof et al., 2010). Another olistolithe comparable to the Roggspitze is the Hasenfluh west of the Flexenpass (SW of label 1 in Fig. 3).

The **Inntal thrust sheet** is built of Hauptdolomit and Kössen Fm., which are stacked several times. The contact of the Kössen Fm. to the underlying Hauptdolomit is not a stratigraphic contact, as the Hauptdolomit is folded below the straight contact (E of label 5 of Fig. 5). The hectometric, truncated folds in the Hauptdolomit, the orientation of branch lines in the Inntal thrust sheet and the orientation of the splay thrusts are consistent with an initial NW-directed movement of the Inntal thrust sheet. The Krabachjoch klippen have, however, been refolded with NE-trending folds, which are consistent with those found in the Penninic units underlying the Northern Calcareous Alps.

The **Krabachjoch thrust sheet** has a sedimentary succession reaching from the Lower Triassic Muschelkalk Group to the Upper Triassic Hauptdolomit. The sedimentary facies, and the anchimetamorphic overprint (Petschik, 1989) have been interpreted to indicate an origin from the southern margin of the present-day Lechtal thrust sheet, where comparable facies and metamorphism are present (May & Eisbacher, 1999).

The outcrops in the Flexenpass area show that steep faults that formed during Penninic rifting in the Early Jurassic continued to be active well into the Cretaceous (Monzabon fault) and caused block tilting and associated sliding of blocks. Slide phenomena in the vicinity of the Rüfikopf and the megabreccia of the Trittalpe document this stage of passive-margin evolution. With the start of inversion of the continental margin, sedimentary thicknesses were no longer controlled by passive margin architecture, and significantly increased in the synorogenic deposits of the Lech Fm. The first sign of arrival of the Inntal thrust sheet are olistolithes sourced from its tip. The present day geometry of the Krabach klippen is a result of Cretaceous thrust movement overprinted by Paleogene NE-directed transport and folding with NW-trending axes (Erli-Syncline of Fig. 5), and Neogene NW-directed transport and folding with NE-trending axes (Kugla-Syncline of Fig. 5). In spite of the polyphase reactivation of thrusts, the original upper-footwall position of the synorogenic deposits can still be recognized.

3.1.2 Field trip stops

The field trip starts from Lech. The Rüfikopf cablecar brings the group to the Rüfikopf. All other stops are reached by a full day walk to the Trittalpe and the Flexenpass road at Zürs. The field trip route is strongly dependent on weather conditions. It may be necessary to change the route on short notice in case of unfavourable conditions. The positions of all stops are given in Figure 5.

Stop 1, mountain station of the Rüfikopf cablecar (47°12'5.52"N, 10°10'4.14"E)

Geologic trail from the mountain station of the Rüfikopf cablecar to the Monzabonsee. The sedimentary succession from the uppermost Hauptdolomit (Plattenkalk) to the Kössen Fm., Oberrhät

limestone as described in stops 8-10 of Meier et al. (2010). View of the Inntal thrust below the Rüfispitze onto the Lech Fm.

Stop 2, Monzabonsee (47°11'48.18"N, 10°10'12.61"E)

The condensed sedimentary sequence of the Zürs swell spanning the complete Jurassic and most of the Early Cretaceous between the Oberhät limestone and the Lech Fm. is locally represented in a few centimeters of a haematite-rich crust (stop 18 of Meier et al., 2010). In some places Lower Jurassic Adnet Fm. is found in neptunian dykes, and overlying the Oberrhät limestone, testifying block tilting (Fig. 6; stops 11-14 of Meier et al., 2010).

Stop 3, footpath from Monzabonsee to Trittalpe (47°10'51.43"N, 10°10'6.39"E)

View of the Roggspitze olistholith in the Lech Fm., and of the stacked Inntal and Krabachjoch thrust sheets immidiately to the north (Fig. 7).

Stop 4, Trittalpe (47°10'32"N, 10°10'30.84"E)

We cross a "maze" of blocks of Oberrhät limestone, some of which with Kössen Fm. at the base and overlain by deposits of the Zürs swell and Lech Fm., that were emplaced during block tilting and activity of the Monzabon fault. At the base of a lift post at the northern side of the dirt road along the Pazüel creek to the east, a 10 m thick sedimentary succession of the Zürs swell is exposed (Fig. 6).

Stop 5, NW of Pazüelalpe on footpath to Stuttgarter Hütte (47°10'47.18"N, 10°11'14.10"E)

Full view of the folded thrusts of the Krabachjoch klippen.

3.2 Thrust-sheet-top deposits in the vicinity of the Hanauer Hütte

3.2.1 Local geology

The Gosau Group consists of Upper Cretaceous to Middle Eocene clastic syntectonic sediments that are found in the whole area of the Northern Calcareous Alps (e.g., Wagreich & Faupl, 1994), and on top of exhumed Austroalpine basement units (e.g., Neubauer et al., 1995). They overlie a regional erosional and angular unconformity, that truncates structures formed prior to transgression. The Gosau Group is subdivided into a continental to shallow marine Lower Subgroup, and a deep marine, bathyal Upper Subgroup (Wagreich & Faupl, 1994). In the Muttekopf area, breccias of the Gosau Group that formed under continental conditions have a thickness of up to 100 m in the easternmost part (Fig. 7; Haas, 1991). The breccias are overlain by up to 50 m of fossil-rich, neritic marls (*Inoceramus* marls) of Late Coniacian to Early Santonian age (Fig. 8; Leiss, 1990). Another sharp and locally angular unconformity separates the Lower from the Upper Gosau Subgroup, which consists of a up to 1000 m thick succession of sediment gravity flows intercalated with marls.

The deep marine sediments can be grouped into facies associations (e.g., Pickering et al., 1986; Walker, 1975). The most important are a proximal thick-bedded turbidite facies association, and a distal thin bedded turbidite facies association (Ortner, 1994a). The **thick-bedded turbidite facies association** is characterized by dm- to m-bedded sandstones with complete Bouma Ta-Td divisions, which are often amalgamated. In many cases, the turbiditic sandstones develop from conglomerates or breccias by grading. They alternate with light grey to yellow coloured turbiditic marls. The conglomerates and breccias are often matrix-rich and can be very coarse, with blocks with a maximum diameter of 170 m (Fig. 7), in beds several tens of meters thick. In contrast, the **thin-bedded turbidite facies association** consists of cm-thick sandstone beds that contain only the Bouma Tc-interval alternating with black, often laminated marls. Occasionally, dm-thick

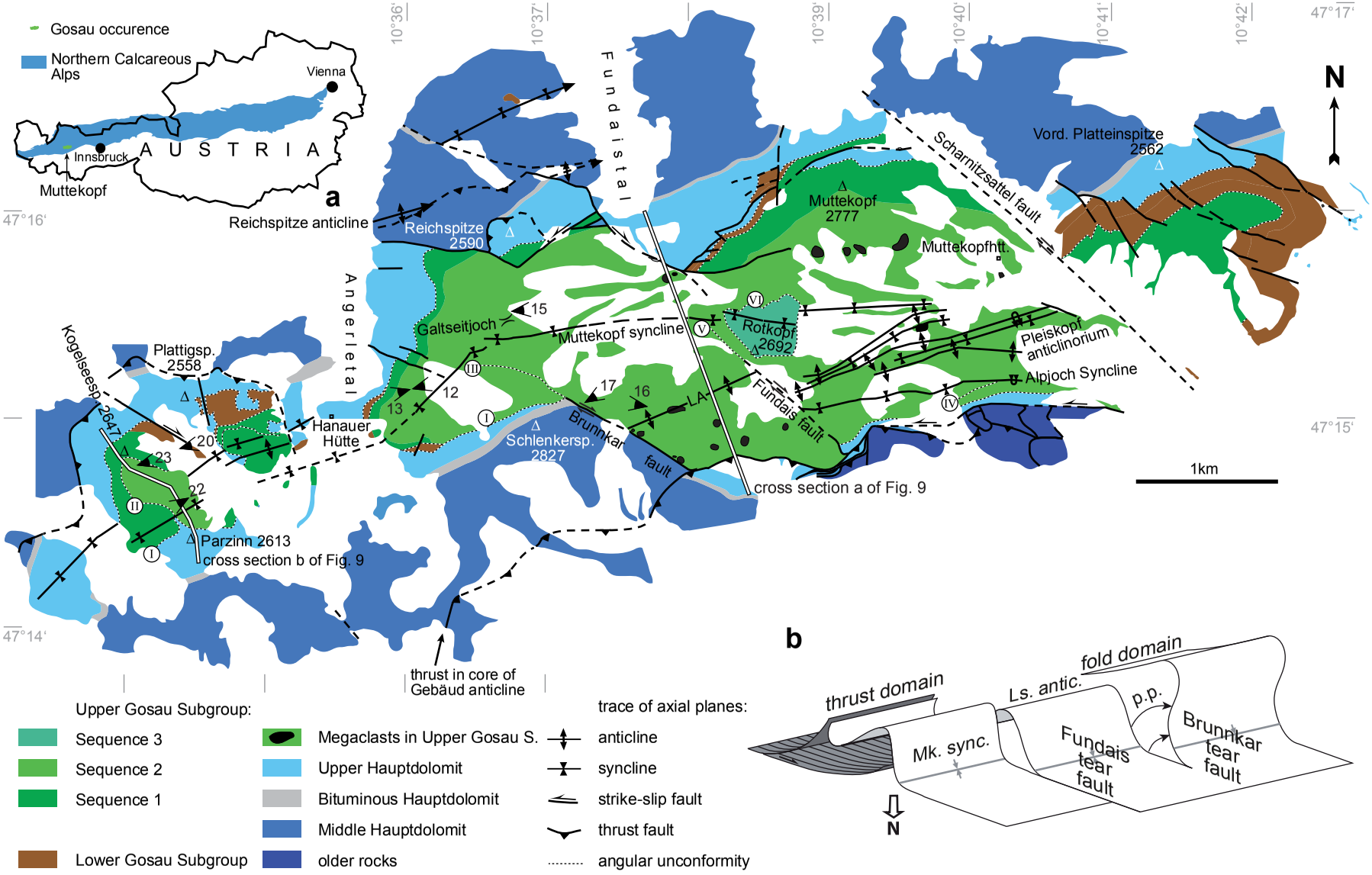

Fig. 7: Geological sketch of the Gosau Group of Muttekopf. Roman numerals indicate angular unconformities: I = Schlenkerspitze unconformity, II = Parzinn unconformity, III = Schlenkerkar unconformity, IV = Alpjoch unconformity, V = Fundais unconformity, VI = Rotkopf unconformity. Eye symbols mark positions from which field photographs with respective figure numbers were taken. Heights in meters. Inset a: Position of Muttekopf Gosau in Northern Calcareous Alps. Inset b: Schematic 3D sketch illustrating the geometry of the Muttekopf syncline, and the Brunnkar and Fundais tear faults separating fold segments with changing wavelength and amplitude. Mk. sync = Muttekopf syncline, Ls. antic. = Larsenn anticline, p.p. = particle path.

sandstones with complete Bouma Ta-Td divisions, and clast-supported breccias are intercalated.

The black marls are calcite-free but contain dolomite, while the yellow marls contain calcite and dolomite. This observation has been interpreted in terms of deposition of the sediment gravity flows below the CCD (Ortner, 1994b), and is consistent with observations in many other Gosau occurrences of the Northern Calcareous Alps (Wagreich & Faupl, 1994). The transition from continental to shallow marine, and then to deep marine conditions documents rapid and large subsidence during deposition, diminishing in the latest Cretaceous (Wagreich, 1991), and documented by the arrival of shallow water detritus in the youngest turbiditic sandstones of the area (Wopfner, 1954).

In the deep marine sediments of the Muttekopf Gosau outcrop, three upward-fining sequences can be distinguished (Fig. 8). From base to top, the amount of locally derived material diminishes in relation to "exotic" material transported from distant sources (e.g., crystalline pebbles) in clast composition and heavy minerals (Ortner, 1994a, b). This documents progressive burial of pre-existing topography and transgression onto large parts of the Northern Calcareous Alps. Many coarse-grained beds can be traced all across the syncline, and can be identified in all parts of the outcrop (e.g. the "white bed" marker, Fig. 8) (Amerman, 2009), unless the beds lap out against an unconformity. Deposition took place in a confined basin (Sinclair & Tomasso, 2002), primarily controlled by the growth of the Reichspitze and Gebäud anticlines (Fig. 7) northerly and southerly adjacent to the Muttekopf syncline in which the Gosau Group is preserved. Active fold growth during deposition did cause instability of the sea floor and promote all kinds of slump deformation at the sediment surface, but also subsurface sediment mobilization (Ortner, 2007). The majority of sediment gravity flows were deviated into the direction of the fold axis of the Muttekopf syncline, and only a relatively small number of flows down the limbs of the syncline were recorded (Ortner et al., 2015).

Cretaceous thrusting in the Northern Calcareous Alps was transpressive (e.g., Linzer et al., 1995; Wagreich, 2001), and therefore the thrust sheets are dissected by numerous tear faults that terminate against the thrusts (Eisbacher & Brandner, 1995, 1996). In the field trip area, these are regularly 1.5 km spaced. East of the Hanauer Hütte, the Brunnkar tear fault offsets the southern limb and ends near the core of the Muttekopf syncline, while the Fundais tear fault offsets the both limbs (Fig. 7). Both faults are very pronounced in the pre-orogenic sediments, but disappear within the syn-tectonic sediments of the Gosau Group. The sediment geometries in the vicinity of the tip of the Brunnkar tear fault are one of the targets of this field trip.

The segmentation of the Muttekopf syncline has important consequences for the architecture of the syntectonic deposits: The tear faults delimit fold segments with different wavelength and amplitude (inset b of Fig. 7), and therefore the relationship between the rates of vertical structural growth and deposition varies. In the depocenter of the basin east of the Fundais tear fault, where the rate of deposition is high and the wavelength and amplitude of folding is smaller, as structures are related to blind thrusts with folds at their tips (thrust domain of inset b in Fig. 7), Sequence 2 overlaps the folds of the Pleiskopf anticlinorium (Fig. 7). Between the Fundais and the Brunnkar fault, the anticlinorium is replaced by the Larsenn

Fig. 8: Column sections from the Muttekopf Gosau outcrop in the northern limb of the Muttekopf syncline unaffected by major structural growth and related unconformities. Section Plattein: Gully west of Vorderer Platteinspitze, section Muttekopf: Muttekopf north ridge. section Galtseitjoch: Ridge from Reichspitze to Galtseitjoch, section Kogelseespitze: Ridge from Kogelseespitze to Gufelseejoch. Section Plattein and Muttekopf adapted from Haas (1991), sections Galtseitjoch and Kogelseespitze adapted from Ortner (1990). See Figure 7 for locations. Left column: facies associations, middle column: grain size, given according to the scale by Wentworth (1922), right column: heavy minerals. Abbreviations: CC = Calcareous nannofossil zones determined by Wagreich (pers. comm. 1993-1995) and Lahodinsky (1988). Ages from calcareous nannoplancton are in accordance with ages from foraminifera by Oberhauser (1963) and Dietrich & Franz (1976). ↑ = and younger. LGS = Lower Gosau Subgroup, UGS = Upper Gosau Subgroup, sdst = sandstone, t = turbidite, fc = facies. Inset (a): Simplified general stratigraphy of the Gosau Group of Muttekopf.

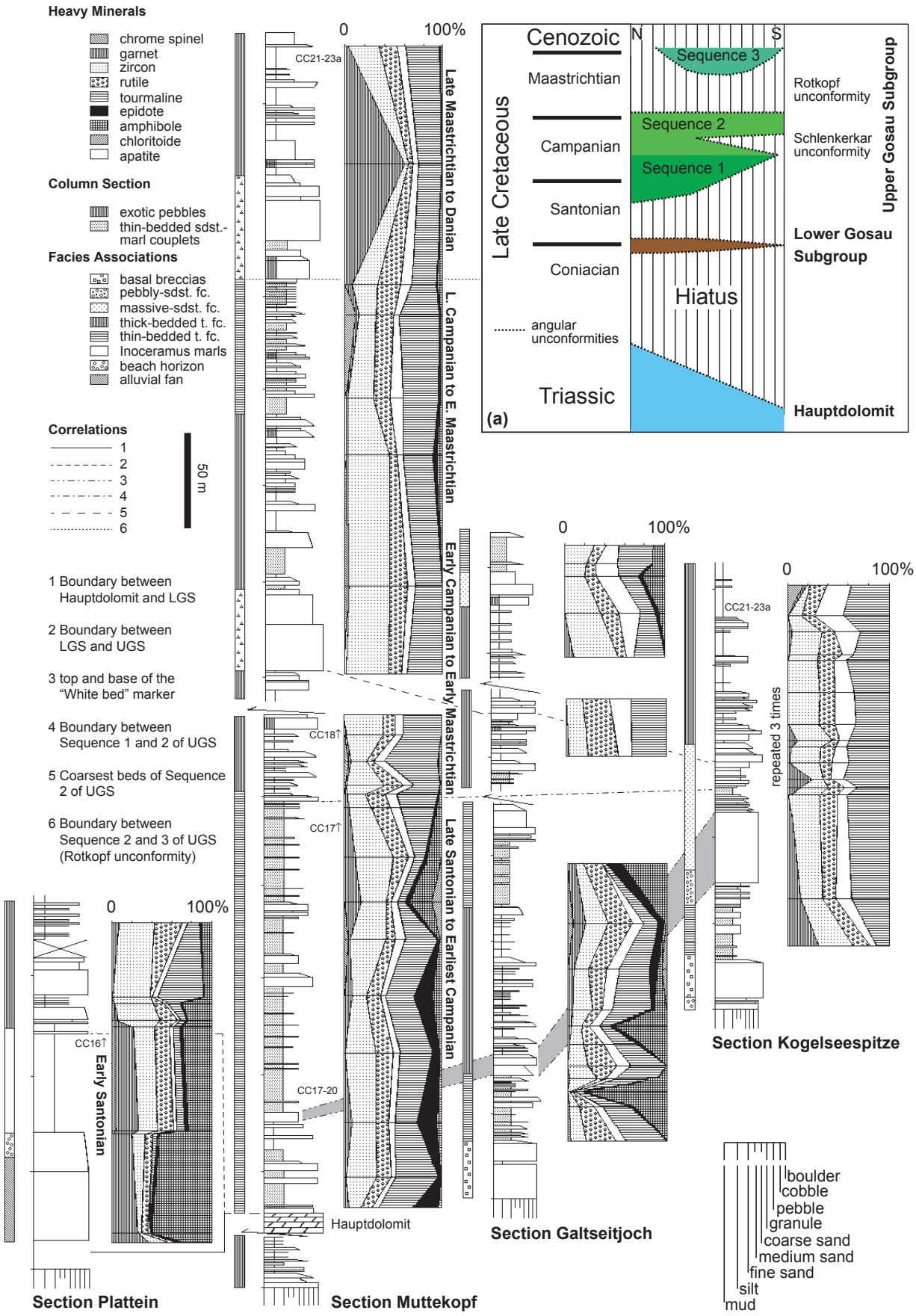
Heavy Minerals
chrome spinel
garnet
zircon
rutile
tourmaline
epidote
amphibole
chloritoide
apatite
Column Section
exotic pebbles
thin-bedded sdst.-marl couplets
Facies Associations
basal breccias
pebbly-sdst. fc.
massive-sdst. fc.
thick-bedded t. fc.
thin-bedded t. fc.
Inoceramus marls
beach horizon
alluvial fan
Correlations
1
2
3
4
5
6
50 m
1 Boundary between Hauptdolomit and LGS
2 Boundary between LGS and UGS
3 top and base of the "White bed" marker
4 Boundary between Sequence 1 and 2 of UGS
5 Coarsest beds of Sequence 2 of UGS
6 Boundary between Sequence 2 and 3 of UGS (Rotkopf unconformity)
Cenozoic
Late Cretaceous
Maastrichtian
Campanian
Santonian
Coniacian
angular unconformities
Triassic
(a)
N
S
Sequence 3
Sequence 2
Sequence 1
Rotkopf unconformity
Schlenkerkar unconformity
Upper Gosau Subgroup
Lower Gosau Subgroup
Hiatus
Hauptdolomit
0
100%
CC21-23a
Late Maastrichtian to Danian
L. Campanian to E. Maastrichtian
Early Campanian to Early Maastrichtian
Late Santonian to Earliest Campanian
CC18↑
CC17↑
CC17-20
CC16↑
Early Santonian
repeated 3 times
Hauptdolomit
Section Plattein
Section Muttekopf
Section Galtseitjoch
Section Kogelseespitze
boulder
cobble
pebble
granule
coarse sand
medium sand
fine sand
silt
mud

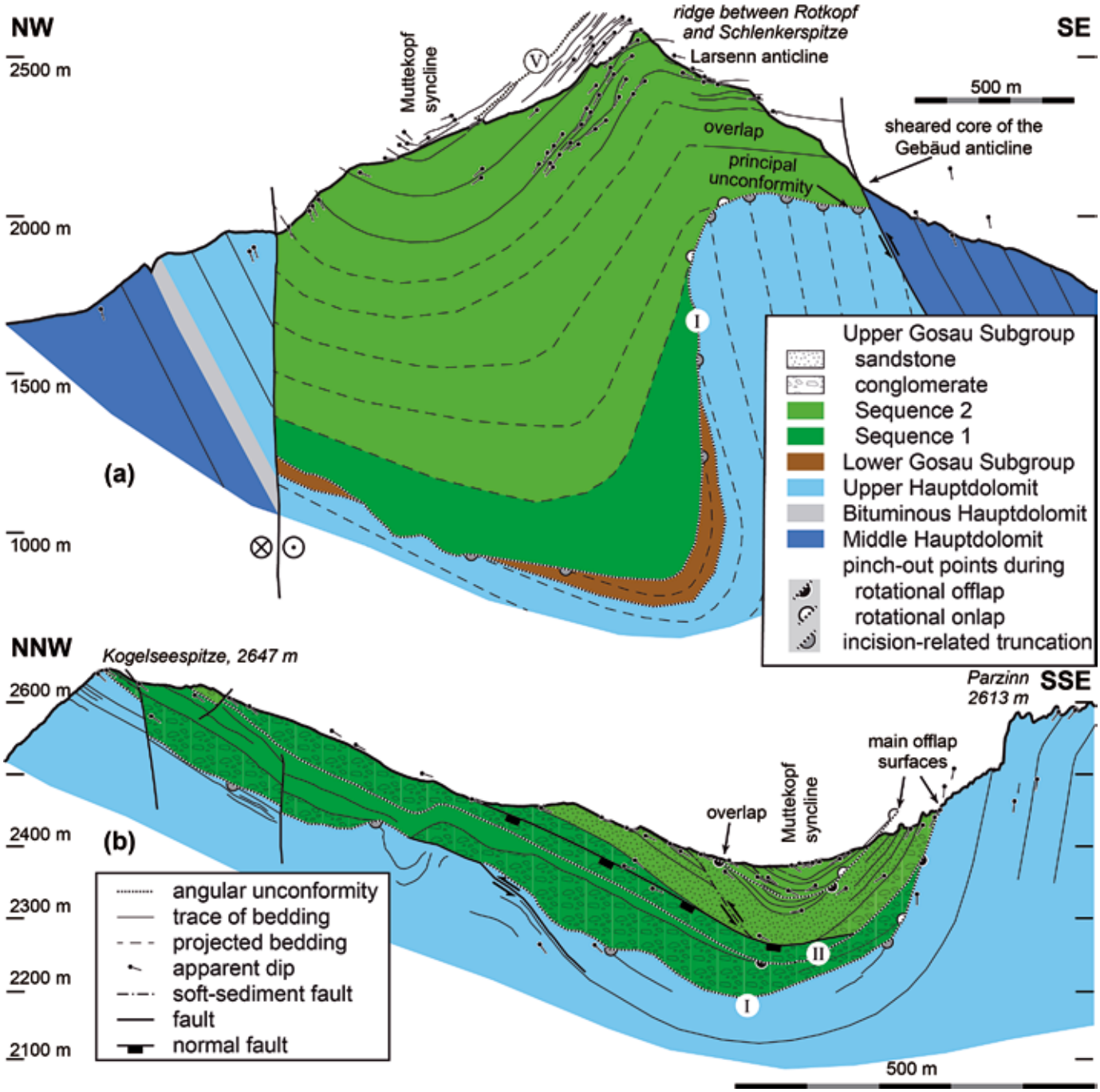

Fig. 9: Cross sections of the Gosau Group at Muttekopf (modified from Ortner et al., 2015). See Figure 7 for location. Angular unconformities: I = Schlenkerspitze unconformity, II = Parzinn unconformity, V = Fundais unconformity. (a) Cross section near the depocenter of the basin. Geology in lower part projected more than a kilometer parallel to the fold axis from the western flank of the Schlenkerspitze-Reichspitze ridge. (b) Cross section in the westernmost part of the basin along the Kogelseespitze - Parzinn ridge. The core of the syncline in Sequence 2 was projected from the east, while the northern part and below the normal fault was drawn according to the outcrops at the western face of Kogelseespitze.

anticline. There, the steep southern limb of the Muttekopf syncline is erosionally truncated at the Schlenkerspitze unconformity (I in Figs. 7 and 9), and overlapped by Sequence 2 of the Upper Gosau Subgroup. The cross section (a) of Figure 9 shows that the Lower Gosau Subgroup and the Sequence 1 wedge out against this truncation surface in the same steep limb, and therefore the Schlenkerspitze unconformity is the principal progressive unconformity (compare Fig. 4b and Fig. 9a). As a consequence, the axial plane of the Gebäud anticline shifts 500 m to the north in the synorogenic sediments, where it is termed the Larsenn anticline (Figs. 7 and 9a). All beds of Sequence 2 overlap this anticline. In the western part of the outcrop around Kogelseespitze and Parzinn, which is separated by the Brunnkar and two more tear faults from the depocenter (Fig. 7), the rate of deposition was much lower. In the steep southern limb of the Muttekopf syncline, the Gosau succession reaches only a thickness of 150 m or less, compared to more than 450 m in the southern limb south of Galtseitjoch (Amerman, 2009). The stratal pattern of the Gosau in the southern steep limb near Parzinn is characterized by rotational offlap.

Thus, the tear faults separate individual parts of the basin with different relationships between vertical structural growth and deposition. Near the depocenter, Sequence 2 in the southern steep limb of the Muttekopf syncline overlaps, while in the west, Sequence 2 offlaps the Larsenn/Gebäud anticline. However, the most prominent unconformity in the area is the Schlenkerkar unconformity. In contrast to the other unconformities, the Schlenkerkar unconformity is laterally not continuous, but connects with the Brunnkar tear fault in map view (Fig. 7). Ortner et al. (2015) were able to demonstrate that the Schlenkerkar unconformity formed as a consequence of contemporaneous fold growth and tear fault activity, and defined the Schlenkerkar unconformity as the type example of fault-related progressive unconformities. Fault activity causes a vertical step in the steep limb of a fold (see inset b of Fig. 7), which is progressively onlapped by sediments, which are dragged by the fault. This causes bedding to change strike progressively toward the orientation of the tear fault, and dip to decrease upsection, while, for comparison, in classical unconformities related exclusively to fold growth, only dip decreases upsection.

3.2.2 Field trip stops

The field trip will reach the Hanauer Hütte in the evening of day 1. Day 2 will be used to visit the Gosau Group east of the hut at Galtseitjoch and Brunnkar and show the Schlenkerkar unconformity and the Brunnkar tear fault. The Gosau Group west of the Hanauer Hütte will be shown on day 3. There, the smaller rate of deposition has led to the development of a several angular unconformities in both limbs of the Muttekopf syncline. The field trip route is strongly dependent on weather conditions. It may be necessary to change the route on short notice in case of unfavourable conditions. The position of all stops are shown in the detailed maps of Figures 10 and 11.

Stop 6, viewpoint at ridge and turn of path at western side of Schlenkerkar (47°15'5.97"N, 10°36'4.60"E)

On the path from Hanauer Hütte to Stop 6 we cross the Schlenkerspitze unconformity, which is marked by the transition from the Middle Hauptdolomit to conglomerates of the Lower Gosau Subgroup at 2050 m. The unconformity is not directly exposed. At 2080 m we reach the thin-bedded turbidites of the Upper Gosau Subgroup, which are well exposed in a creek at 2130 m. The rest of the path to the viewpoint crosses a grassy slope.

Looking east, the viewpoint offers one of the best views of the Schlenkerkar unconformity. We look directly into the core of the Muttekopf syncline within Sequence 2 of the Upper Gosau Subgroup. Figure 12 indicates the main features to observe: At the Schlenkerkar unconformity (III of Fig. 12), beds converge uphill. The units below the Schlenkerkar unconformity are truncated and overlapped near the ridge, while they are onlapped further down. Thus, the Schlenkerkar unconformity is a true progressive unconformity.

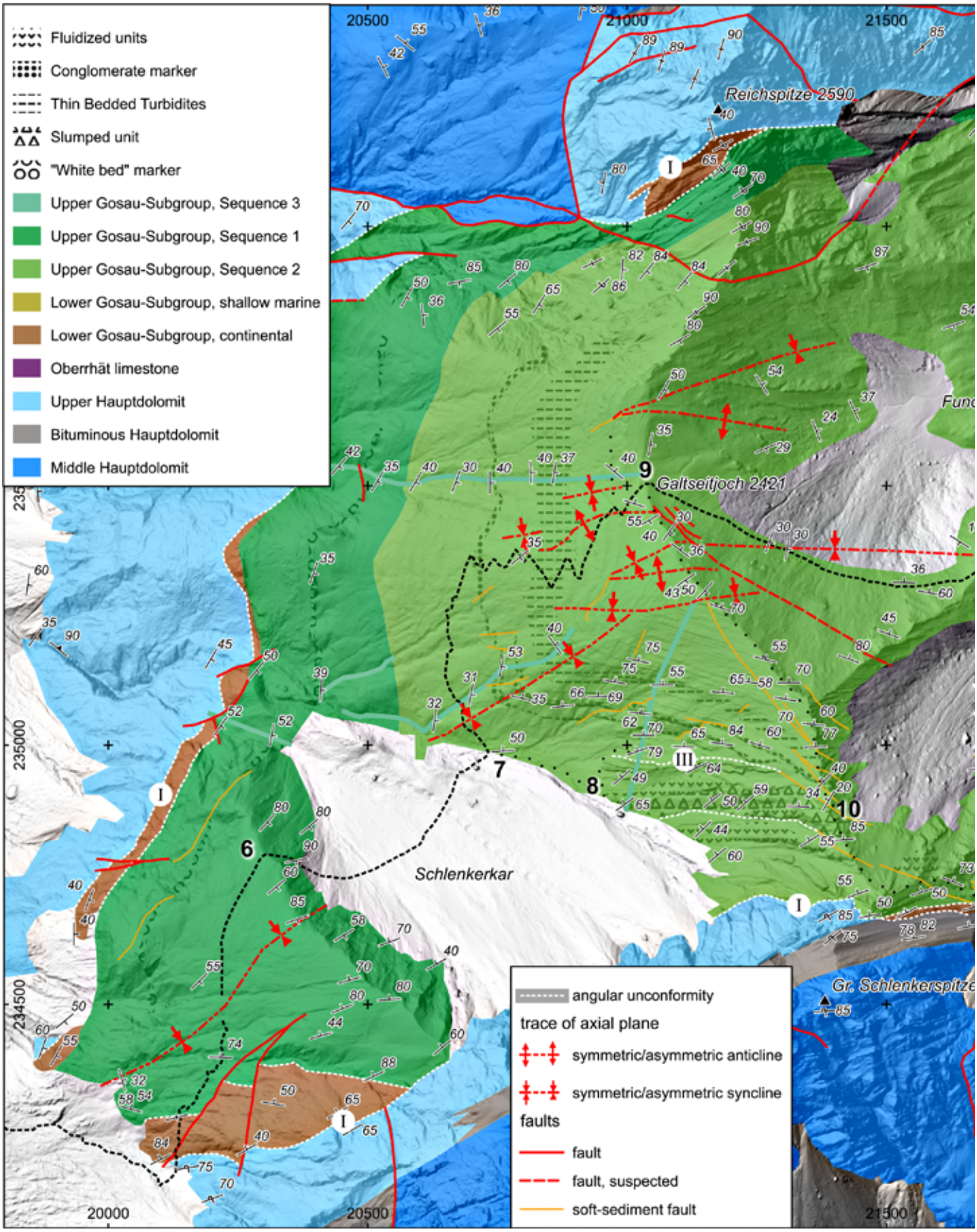

Fig. 10: Detailed geologic map of the field trip area east of the Hanauer Hütte. Numbers 6-12 denote field trip stops. Angular unconformities: I = Schlenkerspitze unconformity, III = Schlenkerkar unconformity, V = Fundais unconformity, VI = Rotkopf unconformity. Graticule: MGI/Austria GK West (EPSG: 31254).

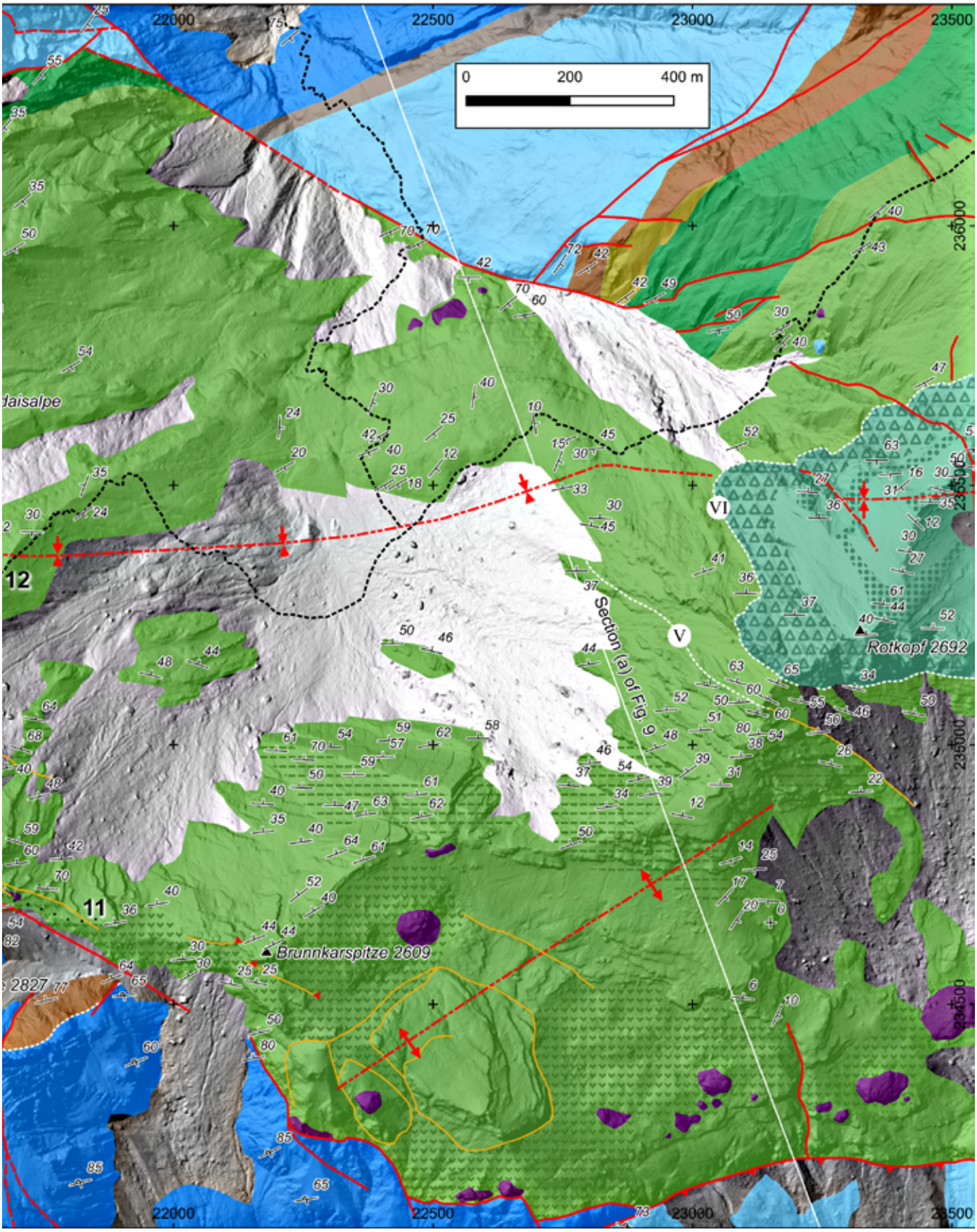
0
200
400 m
22000
22500
23000
23500
Section (a) of Fig. 9
Rotkopf 2692
Brunnkarspitze 2609
2827
11
12
V
VI

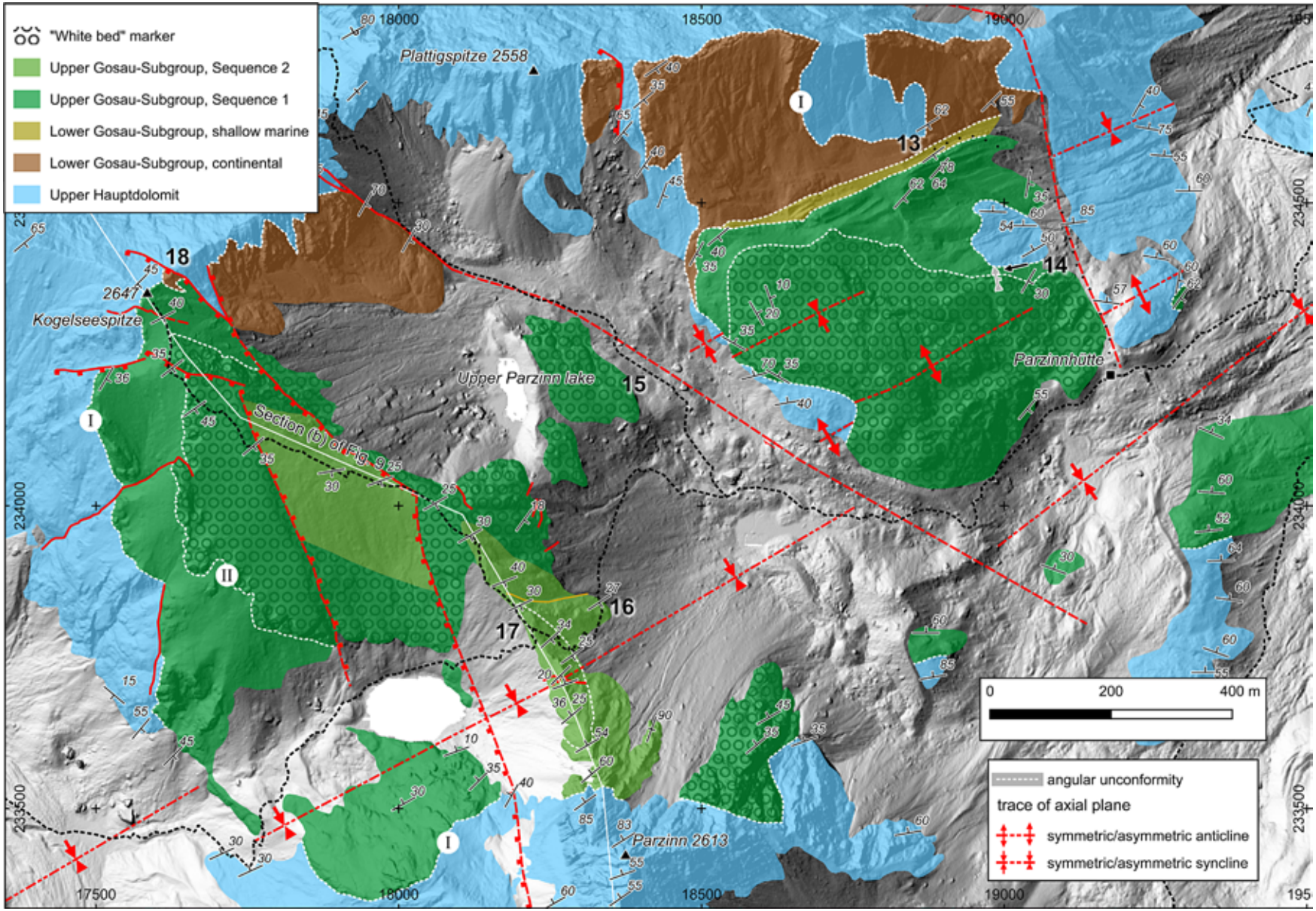

Fig. 11: Detailed geologic map of the field trip area west of the Hanauer Hütte. Numbers 13-18 denote field trip stops. Angular unconformities: I = Schlenkerspitze unconformity, II = Parzinn unconformity. Arrows show style and direction of slump deformation, see legend of Figure 14. Graticule: MGI/Austria GK West (EPSG: 31254).

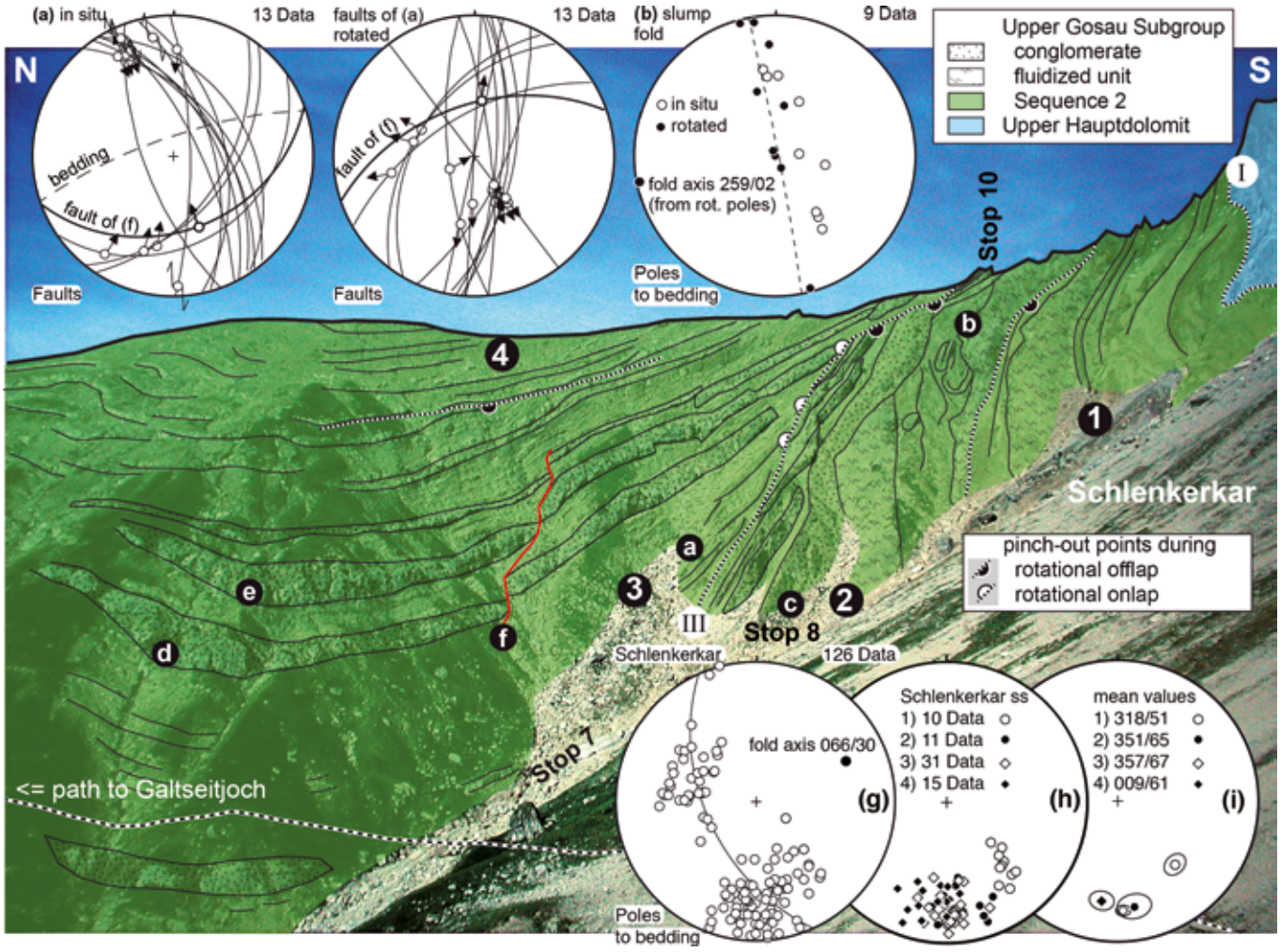

Fig. 12: View to the east at Stop 6. Angular unconformities: I = Schlenkerspitze unconformity, III = Schlenkerkar unconformity. (a) - (f) label geological features that are described in the main text, and, in the cases (a) and (b) also diagrams that show orientation data from the respective outcrops. 1-4 denote domains in the steep southern limb of the Muttekopf syncline separated by angular unconformities. Bedding orientations in diagrams (h) and (i) are shown grouped according to these domains, while diagram (g) gives all bedding orientations and the calculated fold axis from the Schlenkerkar.

The units below the Schlenkerkar unconformity are overprinted by mass wasting. Slump deformation is documented by large slump folds (b of Fig. 12), and by channelized conglomerates and sandstones right below the unconformity. The latter formed in the troughs at the surface of a conglomerate affected by stretching-related pinch-and-swell structures (c of Fig. 12). This bed truncates a composite mass transport complex with fluidized parts and a slump-folded unit inbetween. The fluidized units are easily recognized as they show spheroidal weathering (e.g. bed with label 2 of Fig. 12). Fluidization is documented by injection of conglomerate into the sandstones and marls of the middle unit.

Above the Schlenkerkar unconformity, mass wasting is less important (see Stop 8 for a description of small scale deformation style). In the panorama, a fault with several meters of offset is visible

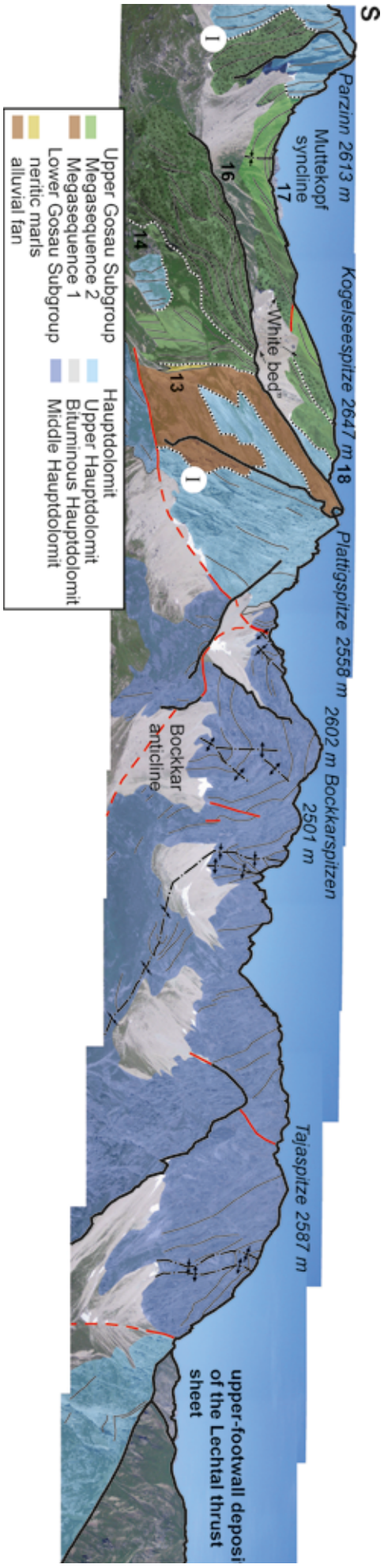

Fig. 13: View to the west at Stop 6. Angular unconformities: I…Schlenkerspitze unconformity. 13, 14, 16, 17, 18 denote field trip stops. The southern limb of the Bockkar anticline is shortened by an out-of-sequence thrust that postdates folding, and has therefore reduced thickness. The axial plane in the core of the Bockkar anticline shifts position by bedding-parallel shearing. Note converging bedding in the Gosau Group south of the Plattigspitze. Further explanations in the text.

(f of Fig. 12) that offsets beds (d) and (e). A staircase pattern of the fault is evident, which has been observed also in other deep water sedimentary systems (e.g., Lansigu & Bouroullec, 2004), and has been predicted by forward modeling (e.g., Schöpfer et al., 2006).

Beds (d) and (e) in Figure 12, and also beds below and above, have their greatest thickness right in the core of the syncline. This documents the existence of folding-related surface topography during deposition. However, topography was small, as the beds are continuous and overlap this topography. For orientation analysis of the Muttekopf syncline in Schlenkerkar, the sedimentary succession in the steep limb of the Muttekopf syncline was divided into four domains separated by angular unconformities, labeled 1-4 in Figure 12. If poles to bedding are split accordingly, a progressive change in bedding orientation from NW-dipping to NNE-dipping becomes evident (diagrams h and i of Fig. 12; see also map of Fig. 10). This is unexpected as unconformities related to fold growth should display a progressive change in dip, and not a change in strike. The progressive change of strike has been interpreted as a consequence of combined folding and tear fault activity (Ortner et al., 2015). The vertical step across the tear fault (see inset b of Fig. 7) is draped by sediment, the sediment then dragged by the fault, and onlapped by younger sediments. This creates a secondary wedge at the upper tip of the tear fault. The relative importance of fold growth versus vertical growth of topography related to tear fault activity controls whether a change of dip or a change of strike is observed at an angular unconformity. In the case of the Schlenkerkar unconformity, vertical growth of topography related to tear fault activity was more important. This is expressed by the progressive steepening of bedding across angular unconformities in the steep limb of the Muttekopf syncline, which must be related to fault drag (see change of bedding orientation from domain 1 to 2 in Fig. 12h and i).

Turning around, the panoramic view to the west gives an overview of the geology of the westernmost part of the Gosau outcrop (Fig. 13). In the

ridge between the summits of the Parzinn and the Kogelseespitze, the asymmetric Muttekopf syncline is exposed. While Sequence 1 has relatively constant thickness, Sequence 2 is reduced to 150 m thickness. The Late Maastrichtian nannoplancton age in the core of the syncline (Fig. 8) indicates an age equivalent to the base of Sequence 3, and thus younger than the youngest deposits of Sequence 2 further east, where a smaller time span is represented by roughly 1000 m of sediment. In the foreground, south of Plattigspitze, bedding in sediments of the Lower and Sequences 1 and 2 of the Upper Gosau Subgroup are seen to converge onto the northern limb of the Muttekopf syncline, documenting growth of the Bockkar anticline (Fig. 13), a western continuation of the Reichspitze anticline (Fig. 7) between the Coniacian and the Campanian. The northern limb of the Bockkar anticline reaches to the northern margin of the Inntal thrust sheet, with two anticline-syncline-pairs in the northern ridge of the Bockkarspitzen and the Tajaspitze, respectively. These are second-order folds verging toward the crest of the first-order Bockkar anticline (Fig. 13).

Stop 7, in the gully to the WNW downward out of Schlenkerkar at 2170 m (47°15'12.36"N, 10°36'26.88"E)

The rocks exposed at this outcrop give a good impression of the thick-bedded turbidite facies association. 30-50 cm thick sandstone beds with complete Bouma sequences alternate with meter-thick yellowish turbiditic marls. The bases of the sandstone beds have tool marks and flute casts indicating W to SW-directed sediment transport (Fig. 14), parallel to the regional fold axis (see diagram g of Fig. 12). The fold axis in a sandstone bed folded into the base of an overlying conglomerate bed (Fig. 14) is sub-parallel to the regional fold axis (see diagram g of Fig. 12) and is verging to the SE. Probably, the fold formed as a consequence of syn-depositional tectonic shortening, as it faces the wrong way for a slump fold moving downslope. However, it would be in accordance with the expected orientation of a parasitic fold; alternatively, it could have been rotated out of the downslope direction by downslope gliding (compare Ortner, 2007).

Stop 8, stratigraphic succession across the Schlenkerkar unconformity (47°15'9.66"N, 10°36'35.76"E)

This stop shows some of the more important rock types mentioned at Stop 6. The start of the section is a fluidized conglomerate with a smooth, rounded surface resembling spheroidal weathering, labeled by (2) in Figure 12, and the section continues to label (a). On top of that bed, a coarse-grained succession follows that is part of the boudinaged and channelized beds below the Schlenkerkar unconformity. A characteristic 2 m thick succession of cm - dm beds of grey coarse sandstones grading to fine sandstones, alternating with yellowish, locally laminated siltstones is found in the upper part of this succession, and can be used as a marker bed. The Schlenkerkar unconformity is the boundary to a marl-dominated part of the succession. Therefore, rotational offlap at the Schlenkerkar unconformity was probably caused by a temporary decrease of the rate of deposition. However, this is only partly reflected by the distribution of the facies associations (Ortner, 1994a). The marly sediments directly overlying the unconformity are part of the thick-bedded turbidite facies association, and not of the thin-bedded turbidite facies association. If the unconformity had formed as a consequence of a decrease of the rate of deposition, one would expect the thin-bedded turbidite facies association onlapping the unconformity (compare Stop 6).

It has been stated above that slump deformation is less important above the Schlenkerkar unconformity. Coarse-grained beds are dissected by faults that are sealed upsection and run into bedding downsection. A sandstone bed right above the Schlenkerkar unconformity is offset by m-spaced faults with dm-offsets (diagram a and label a of Fig. 12). After rotation the faults with bedding to horizontal, they document bedding-parallel stretching roughly perpendicular to the fold axis (diagram g of Fig.12). A reason may be downslope

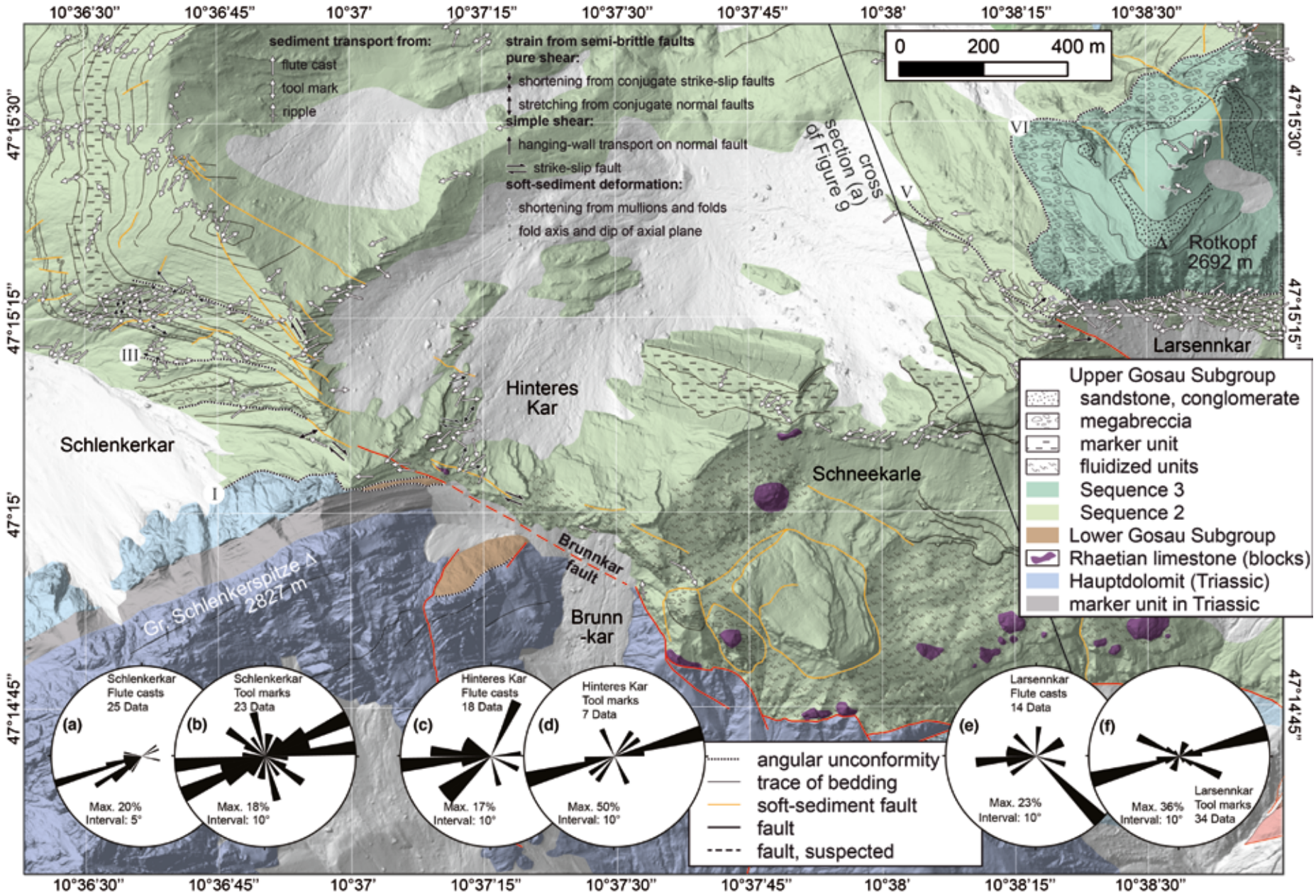

Fig. 14: Sediment transport directions and soft-sediment deformation east of the Hanauer Hütte (modified from Ortner et al., 2015). Angular unconformities: I = Schlenkerspitze unconformity, III = Schlenkerkar unconformity, V = Fundais unconformity, VI = Rotkopf unconformity. (a) – (f) Rose diagrams of flute casts and tool marks. All the sediment transport data have been rotated with bedding to horizontal. Note the dominant sediment transport parallel to the fold axis. A second maximum is developed perpendicular to the fold axis, down the tilting fold limbs. Near the tear faults, sediment transport parallel to the fault (diagram e), or across the fault (diagram c) is seen.

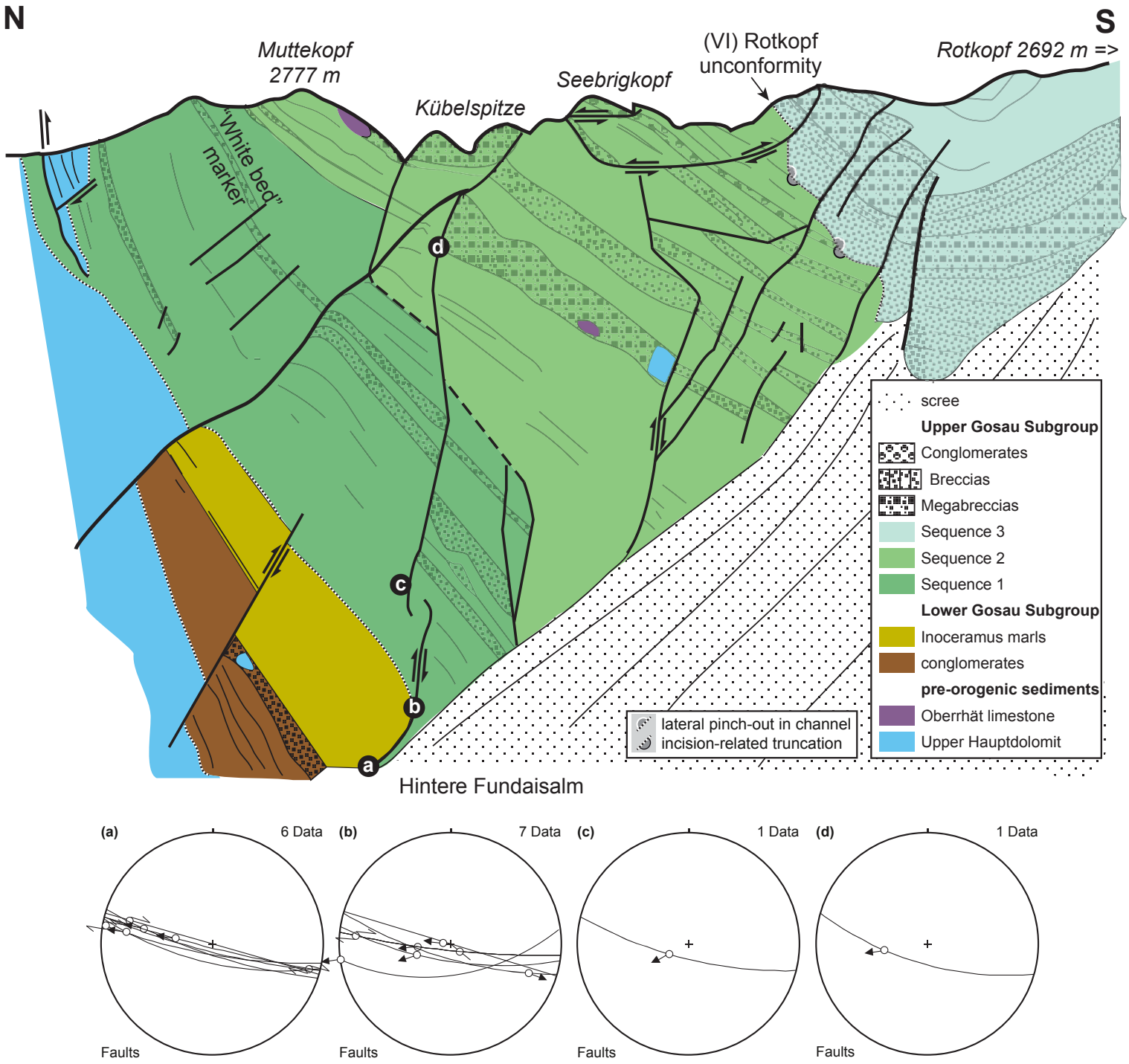

Fig. 15: View to the east of the Kübelwände from Stop 9 at Galtseitjoch (adapted from Ortner, 1994a). Diagrams (a) - (d) show measurements of the Fundais fault (a) and a splay fault at different positions.

gliding after partial lithification during tilting in the southern limb of the Muttekopf syncline. Even if submarine topography related to tilting of fold limbs was very small and was overlapped by single coarse-grained beds, it was sufficient to cause gravitative movement down the limbs of the fold.

Stop 9, Galtseitjoch (47°15'29.06"N, 10°36'39.52"E)

The path to Galtseitjoch crosses the core of the Muttekopf syncline 100 m NW of Stop 6 and then runs in the north limb of the Muttekopf syncline for a vertical distance of 270 m. At 2400 m, the path crosses the core of a secondary anticline.

The marker bed of Stop 8 below the Schlenkerkar unconformity is exposed on the path, and the succession is conformable here. At Galtseitjoch, the thin-bedded turbidite facies association is exposed in a large outcrop 50 m north of the saddle. Current ripples on the upper surface of cm-thick sandstone beds allow to deduce sediment transport to the north or south, while flute casts at the base of dm-thick sandstone beds indicate transport to the SW, parallel to the regional fold axis.

The turbidites of the Upper Gosau Subgroup are largely free of macro-fossils, but trace fossils have been observed occasionally. A bathyal trace fossil association has been documented, and the type of ichnotaxa observed depends on the stability of environmental conditions (Gröger et al., 1997). Trace fossils in the thin-bedded turbidite facies association are therefore ornate feeding traces like *Paleodictyon*, *Spiroraphe*, *Cosmoraphe*, *Desmograpton* and others. *Cosmoraphe* has been found in this outcrop. In the thick-bedded turbidite facies association, *Chondrites*, *Scolicia* and *Nereites* have been observed, which are much more tolerant to changing environmental conditions (e.g., Ekdale, 1985).

The Galtseitjoch outcrop is characterized by open folding with a quarter wavelength of several tens of meters (e.g., north of 9 in Fig. 10). The axial planes of these folds converge and have their origin in thrusts evolving from bedding-parallel movement planes. This smaller scale folding could therefore either be related to submarine mass movements, during which several tens of meters thick successions moved, or to post-depositional out-of-syncline thrusts.

The main attraction at Galtseitjoch is the panoramic view of the Kübelwände below the ridge between the Muttekopf and Rotkopf summits (Fig. 15). At the base of the Kübelwände, a succession of the Lower Gosau Subgroup is exposed (Leiss, 1990). On top, the full succession of the Upper Gosau Subgroup in the northern limb of the Muttekopf syncline is visible. A megabreccia bed of more than 10 m thickness forms the coarsest bed within Sequence 2 between an upward coarsening and a much thicker upward fining part of the succession (see section Muttekopf of Fig. 8). This bed is exposed at the ridge south of the Muttekopf summit, and in the Kübelwände below Seebrigkopf (Fig. 15). The faults offsetting the megabreccia bed are splay faults of the Fundais tear fault (see Fig. 7 for map expression of fault), which has a dextral sense of movement with a normal component that becomes increasingly dip-slip in the younger parts of the Gosau Group (diagrams a - d of Fig. 15). This has been interpreted as a footwall collapse associated with tear fault activity (Ortner et al., 2015).

Sequence 3 cuts into Sequence 2 between Seebrigkopf and Rotkopf at the Rotkopf unconformity (Fig. 15). The coarse-grained base of Sequence 3 is a true channel sidelapping an erosive trough. Incision of this channel was guided by the Fundais tear fault (Ortner et al., 2015). Sequence 3 is preserved in the core of the Muttekopf syncline.

Stop 10, Schlenkerspitze north ridge at 2570 m (47°15'8.33"N, 10°36'56.42"E)

From the Galtseitjoch, we follow the ridge to south toward the Schlenkerspitze. We cross two anticlines and synclines, of which the southernmost is the core of the main Muttekopf syncline. There a dextral fault offsets the southern, but not the northern limb of the syncline. 100 m north of the bifurcation of the ridge at 2540 m this same fault crosses the Schlenkerspitze north ridge. It forms the NE limit of a zone strongly affected by faulting, and which connects with the Brunnkar tear fault to the SE. The outcrop itself is located at a fault that connects with the main Schlenkerkar unconformity. 80 m south of Stop 10, another fault runs into another unconformity (Fig. 10). In the vicinity of the outcrop, subvertical faces of up to 10 m thick conglomerate beds have slickensides with oblique slickenlines.

Right below the Schlenkerkar unconformity at Stop 10, a succession of coarse-grained beds is exposed (Fig. 12), that contains the marker bed mentioned at Stop 8. This documents major stretching of this succession, and interaction of faulting and mass transport processes during offlap, when submarine topography was exposed.

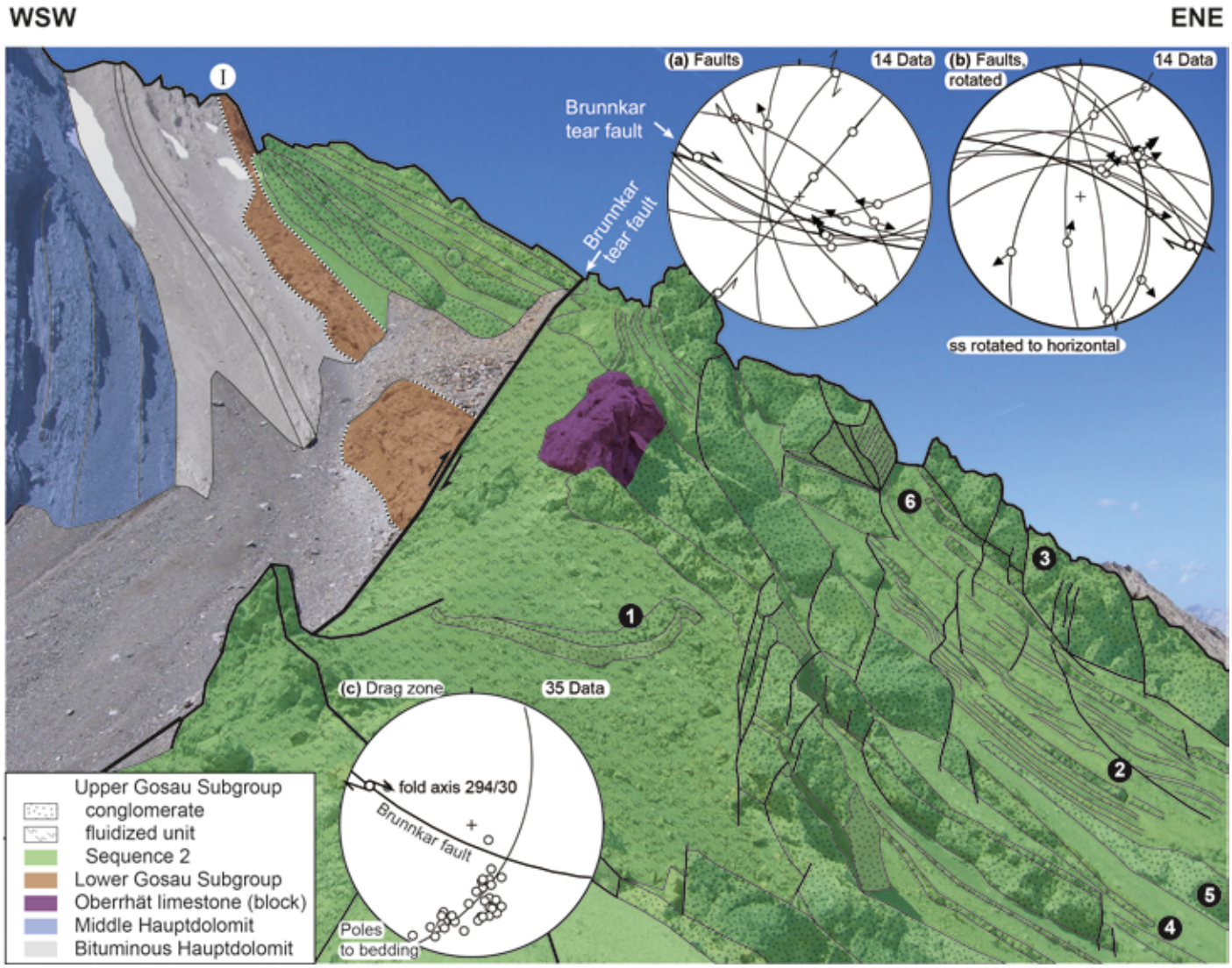

Fig. 16: View to the west of the Brunnkar tear fault and associated deformation in the syntectonic sediments as seen from Stop 11 (modified from Ortner et al., 2015). 1-6 label geological features that are described in the main text. Diagram (a) shows all the faults measured in the drag zone in this outcrop, (b) shows the data after rotation with bedding to horizontal. Diagram (c) shows the poles to bedding within the drag zone and the fold axis calculated.

Stop 11, Brunnkarjöchl between Hinteres Kar and Brunnkar (47°15'1.77"N, 10°37'18.86"E)

We follow the ridge to a secondary summit of the Schlenkerspitze at 2660 m, passing four towers on the rigde on the NE side. The end of the ridge at 2640 m is a large bedding plane, and we use a crevasse to reach the ridge between Schlenkerspitze and Brunnkarspitze. On this ridge we descend 400 m to Stop 11 with a altitude difference of 150 m.

The view to the W is subparallel to the Brunnkar tear fault, that delimits the Hauptdolomit against Sequence 2 of the Upper Gosau Subgroup to the SE, and runs into Sequence 2 to the NW (Fig. 16). On the southwestern side of the Brunnkar tear fault, in the north ridge of the Große Schlenkerspitze, the transition from the thick-bedded Middle Hauptdolomit to the very thin-bedded Bituminous Hauptdolomit is exposed. The latter is a clear marker in the 1800 m thick Hauptdolomit succession. Here I use the subdivision, that was

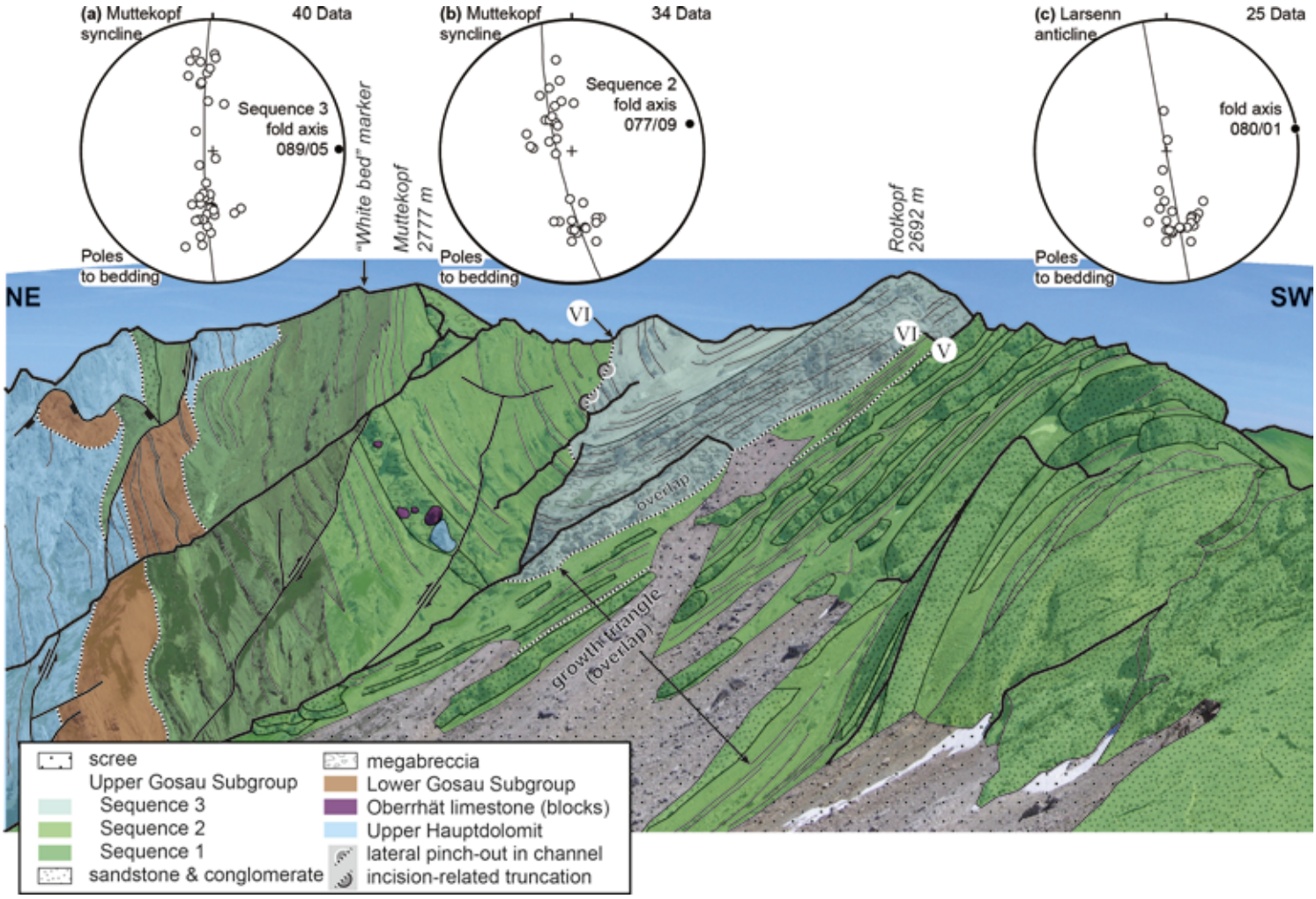

Fig. 17: View to the east, parallel to the axis of the Larsenn anticline, and oblique view of the Kübelwände from Stop 11. Angular unconformities: V = Fundais unconformity, VI = Rotkopf unconformity. Note the growth triangle in the southern limb of the Muttekopf syncline. Draping of the vertical step across the Fundais tear fault and associated change of bedding orientation causes the change in fold axis orientation of the Muttekopf syncline from Sequence 2 (diagram a) to Sequence 3 (diagram b) without a change in shortening direction.

introduced by Müller-Jungbluth (1971) in this part of the Northern Calcareous Alps. It was refined by Donofrio et al. (2003). Unfortunately, this internal organization cannot be recognized in more western (see first part of field trip) and eastern parts of the Northern Calcareous Alps. The Hauptdolomit is unconformably overlain by conglomerates of the Lower Gosau Subgroup, which is in turn unconformably overlain by Sequence 2 of the Upper Gosau Subgroup. Coarse-grained beds in the latter converge upsection (Fig. 16).

On its northeastern side, the Brunnkar tear fault is accompanied by a fluidized unit of varying thickness with slabs of sandstone beds (1 of Fig. 16) and large blocks of Oberrhät limestone. Beds of Sequence 2 are dragged into parallelity to the Brunnkar tear fault (diagram c of Fig. 16; Fig. 10), involving roughly m-spaced faults with oblique slickenlines (diagram a of Fig. 16). Many of these faults run into bedding and cause roll-overs (2 of Fig. 16). Increase of thickness of the beds in the hanging wall of the faults indicate syn-depositional fault activity (3 of Fig. 16). Locally, scarps

of faults are onlapped by conglomerate beds pinching out away from the fault (4 of Fig. 16), and the pinch-out is in turn onlapped by a conglomerate pinching out toward the fault (5 of Fig. 16; compare Pochat & van den Driessche, 2007). Some beds are stacked (6 of Fig. 16). All these features document contemporaneous syn-depositional fault activity, slumping at the sediment surface and onlap of newly deposited sediment on growing submarine topography, and can be compared to trishear normal faulting and associated drag folding (e.g., Gawthorpe & Hardy, 2002).

Turning around, the panorama to the east gives an oblique view of the Kübelwände and the Rotkopf with the Muttekopf syncline (Fig. 17), which has already been discussed at Stop 9. The Larsenn anticline is seen almost exactly parallel to the fold axis. In the steep southern limb of the Muttekopf syncline, the growth triangle (i.e. the zone in which the thickness of syntectonic sediments decreases towards the crest of the anticline) can be recognized, however beds still overlap the anticline. Within the growth triangle, coarse-grained beds are boudinaged and locally stacked because of slump-related deformation. Still within Sequence 2, a decrease in grain-size is seen across the Fundais unconformity, which is another fault-related progressive unconformity related to the Fundais fault. At the base of Sequence 3, the Rotkopf unconformity cuts into Sequence 3 in the northern limb of the Muttekopf syncline, but shows apparent overlap in the southern limb. This is because the SW face of Rotkopf is parallel to the long axis of the channel in which Sequence 3 was deposited.

In the southern face of the Brunnkarspitze, the megabreccia bed comes to the surface in the crest of the Larsenn anticline, with several large blocks of Oberrhät limestone and huge slabs of Upper Gosau Subgroup deposits. Between the summit of Brunnkarspitze and the megabreccia, the fluidized unit that marks the trace of the Brunnkar fault, truncates breccia beds to the south, and the megabreccia bed to the north. To the east, this unit widens dramatically in the crest of the Larsenn anticline, and is exposed over several square kilometers (Figs. 10, 14).

Stop 12, E of Galtseitjoch at 2350 m at the crest of the Muttekopf syncline (47°15'8.33"N, 10°36'56.42"E)

We return to the Galtseitjoch on the way we ascended, or across the blocky Hinteres Kar. 700 m E of the Galtseitjoch where the path crosses a minor ridge, it crosses the core of the Muttekopf syncline. On the NE side of this ridge, large, meter-sized sole marks are exposed at the base of a 2 m thick sandstone bed, that is intercalated in a heterolithic succession of the thin-bedded turbidite association. These have been interpreted as soft-sediment mullions by Ortner (2007). Soft-sediment mullions are "elongate, slightly irregular bulges at the base of coarse-grained clastic beds (sand to conglomerate), separated by narrow, elongate flames of fine-grained material (mud) protruding into the coarse-grained bed" (Ortner, 2015), and should therefore have a subcylindrical, linear geometry, in contrast to the circular to polygonal geometry of load casts. The orientation analysis of the sole marks has shown that both a small circle distribution and a great circle distribution of the bedding poles is present (Fig. 18). The small circle distribution suggest a formation of the structures as load casts, while the preferred orientation of some very steep data may indicate an overprint related to early, bedding-parallel shortening.

Stop 13, Succession of the Gosau Group W of Hanauer Hütte below Plattigspitze (47°14'59.30"N, 10°34'56.58"E)

On day 3, we explore the Gosau Group west of the Hanauer Hütte. We follow the path toward Kogelseespitze and leave it near the Parzinnhütte to go to the north towards the Plattigspitzen.

In a gully south of the Plattigspitzen ridge, the Gosau Group succession starts with a few meters of a monomict, crudely bedded conglomerate with Hauptdolomit clasts. Overlying are dm-bedded, sometimes laminated, light yellow marls that contain small fragments of *Inoceramus* shells, which belong to the *Inoceramus* marls of the Lower Gosau Subgroup. The underlying conglomerates must therefore be part of the Lower

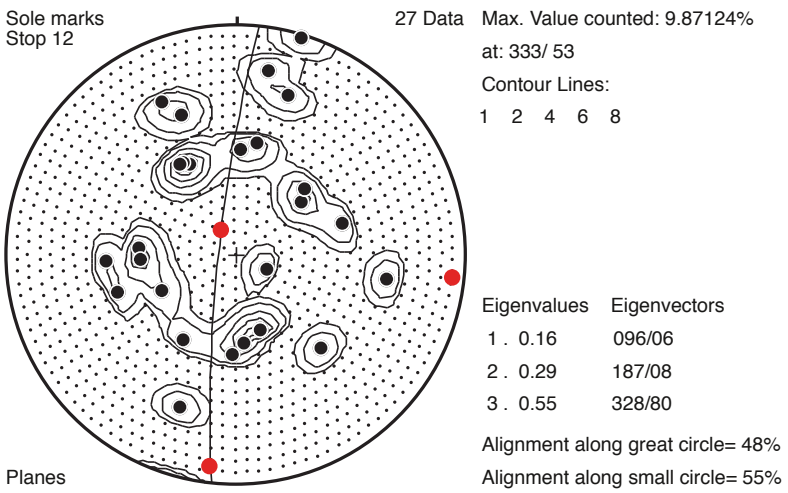

Fig. 18: Bedding orientation at the base of a coarse-grained bed with sole marks at Stop 12. Mean bedding is horizontal.

Gosau Subgroup as well. A sharp boundary separates the *Inoceramus* marls from overlying trace-fossil rich, turbiditic marls of Sequence 1 of the Upper Gosau Subgroup. This boundary is an angular unconformity, and the *Inoceramus* marls pinch out to the SW (Fig. 13).

Sequence 1 below the "White bed" marker onlaps a "paleocliff" of Hauptdolomit north of the *Inoceramus* marls and looses thickness to the WSW rapidly, until it laps out to the south as seen on the other side of the hill (see Stop 15). South of the Plattigspitze and the Kogelseespitze the "White bed" marker is developed as a "distinctive light-colored, clast-supported, dolomite-dominated, pebble conglomerate bed, that can be traced across most of the basin" (Amerman, 2009). In the Plattigspitze-Kogelseespitze part of the basin, this unit consists of a series of deposition events. From Stop 13, the internal architecture of the "White bed" marker can be seen. Laterally stacked channels erode into underlying fine-grained sediments (Parzinn unconformity).

Stop 14, Slump deformation below the Parzinn unconformity (47°14'59.32"N, 10°34'56.48"E)

On the way back, right below the unconformity at the base of the "White bed" marker, slump deformation in thick, yellow, turbiditic marls of Sequence 1 is exposed. Meter-scale duplexes document WSW-directed gliding of the marls (diagram a of Fig. 19), roughly parallel to the fold axis of the Muttekopf syncline. In a nearby rivulet, a m-scale similar style, tight fold in the marls with an oblique, folded stretching lineation on the bedding planes is exposed. A foliation is parallel to the upper limb. As the fold closes to the NE, slump transport was probably to the SW (diagrams b and c of Fig. 19). The folded stretching lineation lies on a great circle (π-circle lines in Fig. 19), and not on a small circle with the fold axis as a center (light grey, bold line in Fig. 19), which is also indicated by the "alignment along great circle" index being larger than 50% (see Wallbrecher, 1986). Such a relationship between a lineation and a fold can be achieved when the folding

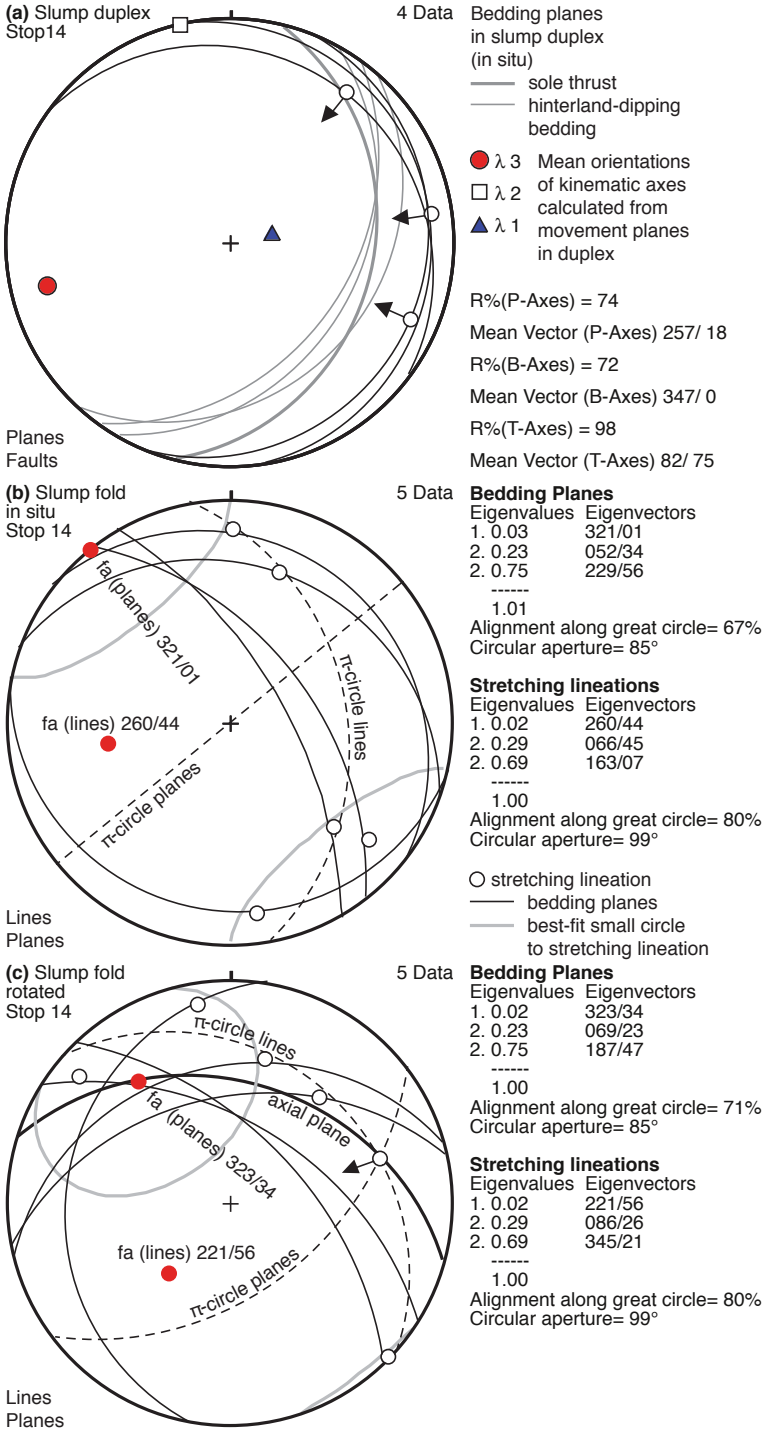

Fig. 19: Orientation analysis of slump structures at Stop 14. (a) Slump duplex in marls. Grey lines give orientation of sole thrust and bedding in slices, respectively. Faults show the transport directions of the slices, which is the direction perpendicular to the intersection of the sole thrust and bedding in the slice. Transport directions were calculated after rotation of bedding to horizontal. Mean transport direction is given as mean orientation of P-axes calculated from the faults. (b) and (c) Slump fold, in situ and rotated to horizontal with local bedding, respectively. Stretching lineations are shown on great circles of bedding. Stretching lineation is oblique to the fold, and distributed along a great circle (π-circle lines), and not along a small circle (grey small circle). This indicates that the fold formed by simple shear, and not by flexural slip, and in such cases, the intersection lineation of the axial plane of the fold and the π-circle of the lines gives the orientation of the shear vector (Ramsay, 1960; Ramsay & Huber, 1987). The direction of shear is interpreted from the closure of the fold to the NE, leading to a SW-directed movement (arrow in c).

process was governed by simple shear parallel to the axial plane of the fold (Ramsay, 1960). In such cases, the intersection between the axial plane of the fold and the π-circle of the lineations gives the transport direction of the fold (Ramsay & Huber, 1987; arrow in Fig. 19c), which is remarkably consistent with the WSW transport direction from the duplex.

Stop 15, Unconformities south of the Plattigspitzen seen from below Oberer Parzinnsee (47°14'46.62"N, 10°34'30.91"E)

We return to the footpath at Parzinnhütte and continue towards Kogelseespitze to the point, where the path to Kogelseescharte and Gramais branches off. We follow this path to the NW until ca. 2250 m.

Looking to the ENE, we see the Parzinn syncline-anticline pair in the Upper Hauptdolomit,

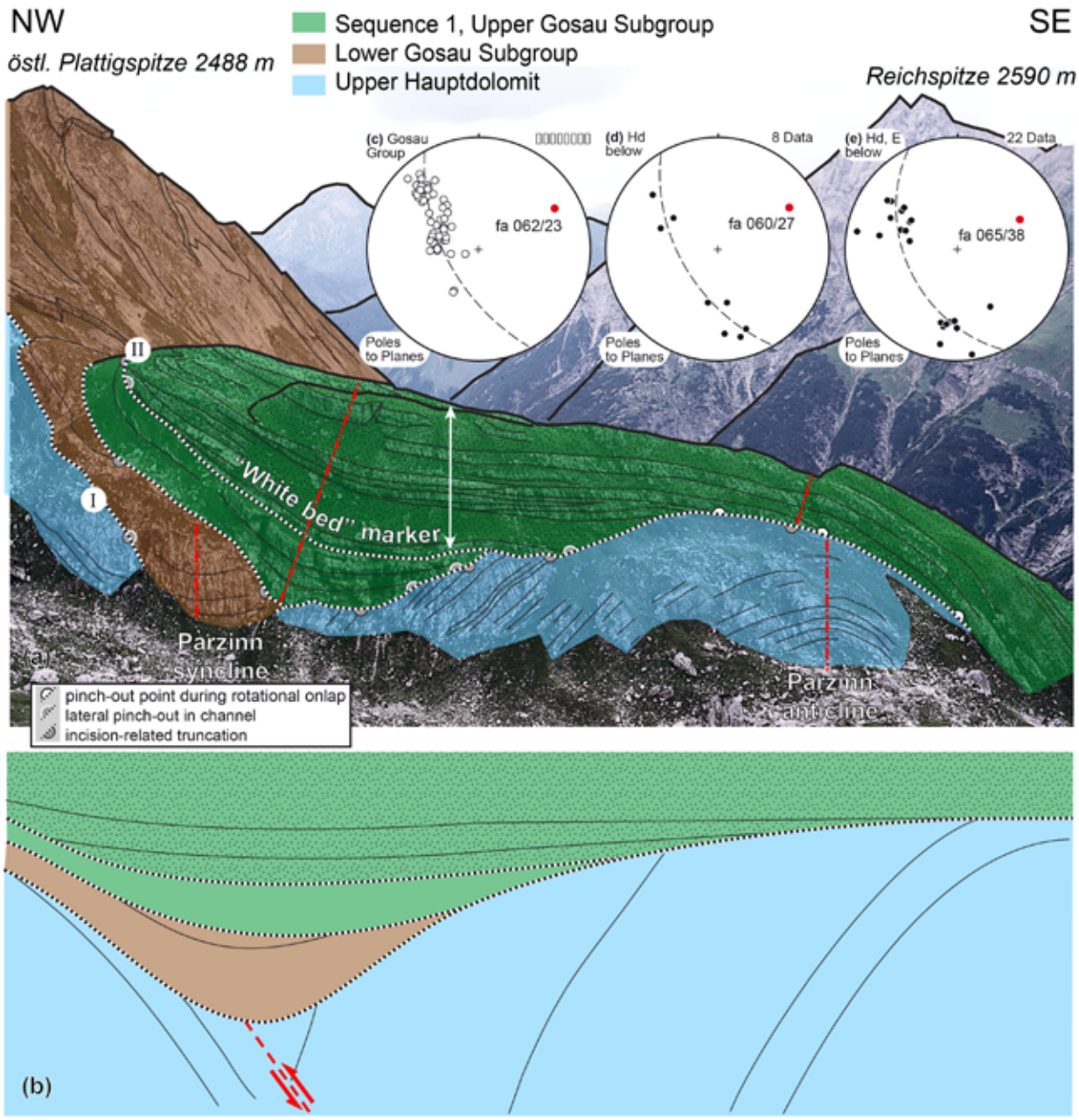

Fig. 20: View to the east at Stop 15 (modified from Ortner, 2001). (a) A fold in the Hauptdolomit is sealed by Gosau Group sediments. Three successive incision events, each documented by an angular unconformity (I = Schlenkerspitze unconformity, II = Parzinn unconformity), lead to a small total thickness of the Gosau Group sediments. (b) Restoration of the youngest Gosau Group sediments to horizontal shows that the field observation of (a) can be explained by a secondary (fault-related?) fold in the northern limb of the Muttekopf syncline. Diagram (c) Bedding poles of Gosau Group sediments south of Plattigspitze. Diagram (d) Bedding poles of Hauptdolomit of Parzinn anticline and syncline as seen in (a). Diagram (e) Bedding poles of Hauptdolomit of Parzinn anticline and syncline east of Stops 13 and 14 (see Fig. 13). Note that fold axes in the syntectonic Gosau Group and in the pretectonic Hauptdolomit are parallel, and not influenced by tear fault activity.

overlain by Gosau deposits with progressively less folding in younger sediments (Fig. 20a; first described by Wopfner, 1954), that elucidate the kinematic history of the folds exposed. The syncline in the north is completely sealed by coarse-grained beds of the Gosau Group, whereas the anticline is progressively onlapped from the NW. In detail, the syncline is filled by conglomerates of the Lower Gosau Subgroup that continue to the north onto the southern flank of the Plattigspitze. The conglomerates show slightly less folding (Fig. 20a). Conglomerates of Sequence 1 of the Upper Gosau Subgroup, however, erosionally truncate the Lower Gosau Subgroup and onlap the Hauptdolomit in the northern limb of the anticline, thereby shifting the local depocenter towards the anticline. Subsequently, the "White bed" marker progressively fills and onlaps the remaining topography related to the growing anticline.

Combining the observations from this stop and Stop 13, three successive incision events can be distinguished: (1) Incision of the Hauptdolomit, when tilting of the northern limb of the Parzinn anticline had started. (2) Incision at the top of the Lower Gosau Subgroup in the Parzinn syncline, and of the Hauptdolomit in the Parzinn anticline. The latter probably experienced more uplift during growth of the anticline, and the Lower Gosau Subgroup was removed by erosion. (3) Incision at the base of the "White bed" marker, that removed all fine-grained Sequence 1 deposits that are preserved further east (Stop 14, Fig. 13). During deposition of the topmost beds of the "White bed" marker, growth of the Parzinn anticline and syncline had ceased. This stage is depicted in Figure 20b. The pinch-out of these beds toward the S also in the southern limb of the Parzinn anticline may indicate (1) that this fold limb, and topography on top was dipping to the north during deposition, or (2) that the axial plane of the Parzinn anticline has in fact a shallow dip to the N, so that only the northern limb of the anticline was exposed.

Ortner et al. (2015) reported a fold system in a comparable structural position in the northern limb of the much larger Muttekopf syncline in the western face of the Kogelseespitze, which is also sealed by the "White bed" marker. There, the axial planes dip to the north, and the fold formed above a thrust cutting upsection to the north. The Parzinn fold system is therefore a secondary fold related to an out-of-syncline thrust that formed in a very early stage of folding of the larger Muttekopf syncline during deposition of the Lower Gosau Subgroup and the lower part of Sequence 1 (see restoration of Fig. 20b), and therefore in the Coniacian to Early Santonian.

Unlike in the Schlenkerkar - Galtseitjoch area, the fold axes of all folds in the Hauptdolomit and the Gosau Group are parallel (diagrams c, d and e of Fig. 20). This documents that the deposits and folds in the Parzinn-Plattigspitze area were not influenced by tear fault activity. Growth of the structures observed in this part of the basin is therefore only related to tilting of fold limbs.

Stop 16, Soft-sediment folding at 2340 m at the eastern side of Gufelseejöchl (47°14'32.63"N, 10°34'28.30"E)

We return to the path towards Kogelseespitze and follow this path to the lowest cliffs south of the path. There, a meter-scale, NW-verging anticline and syncline is exposed in a succession of dm-bedded sandstones alternating with cm-thick marls in the northern limb of the Muttekopf syncline slightly north of the core of the fold (Fig. 21). In the core of the anticline, soft-sediment mullions formed at the base of sandstones where in contact with marls (1 of Fig. 21). Soft-sediment mullions most commonly are found in fold cores (Ortner, 2007, 2015). The laminated marls in the core of the anticline are thickened by duplex formation (2 of Fig. 21). Below a overlying conglomerate bed, a thrust parallel to bedding in the SE limb of the anticline dissects the steep NW-limb and causes an isoclinal fold in a sandstone bed (3 of Fig. 21). While the fold below this thrust must have formed by flexural slip folding, the sandstone bed in the isoclinal fold above the thrust must have progressively rolled through the hinge of the fold.

The soft-sediment mullions, frequent duplex formation, and formation of isoclinal folds give

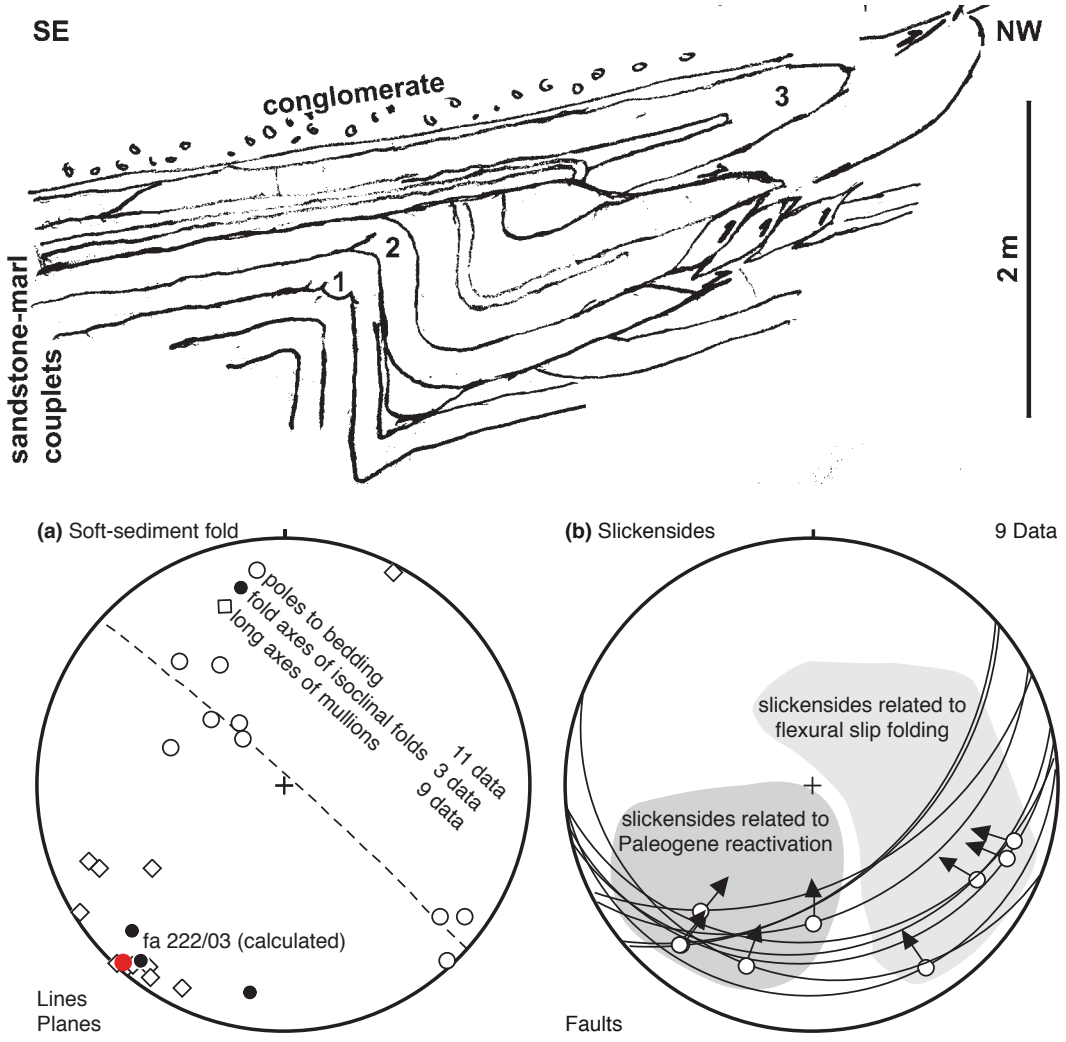

Fig. 21: Field sketch of a NW-verging soft-sediment fold at Stop 16. 1 = soft-sediment mullions in core of fold, 2 = location of small scale stacking with ramp-flat geometry in marls. 3 = isoclinal fold in sandstone bed formed at the tip of a long-limb thrust. Diagram (a) Orientation analysis of fold elements. The long axes of soft-sediment mullions and the isoclinal fold are parallel to the fold axis calculated from bedding planes, and therefore probably cogenetic. Diagram (b) Bedding-parallel slickensides record flexural slip folding and younger reactivation during (minor?) Paleogene fold growth. Further explanations in the text.

evidence of formation of the fold prior to final lithification. The fold axis of this fold is parallel to the the long axes of mullions and of isoclinal folds in the outcrop (diagram a of Fig. 21), and to the axis of larger scale folds (e.g., diagrams c - e of Fig. 20) that formed during deposition of the Gosau. Therefore this is a rare example of a fold in which soft-sediment tectonic shortening can be demonstrated.

Some bedding-parallel slickensides in the fold are perpendicular to the fold axis (diagram b of Fig. 21) and in agreement with flexural slip folding. Another group is, however, sub-parallel to the fold axis. This group of slickensides is not accompanied by soft-sediment deformation features and therefore postdates growth of the Muttkopf syncline. In his analysis of growth folding in the Muttekopf area, Ortner (2001) found that approximately 20% of the folding in the Muttekopf syncline postdates deposition of the Gosau Group, which must be Paleogene and younger. This shortening has a NE-SW direction (see chapter 2), and is in agreement with the orientation of this second group of slickensides and documents late stage tightening of the existing km-scale folds.

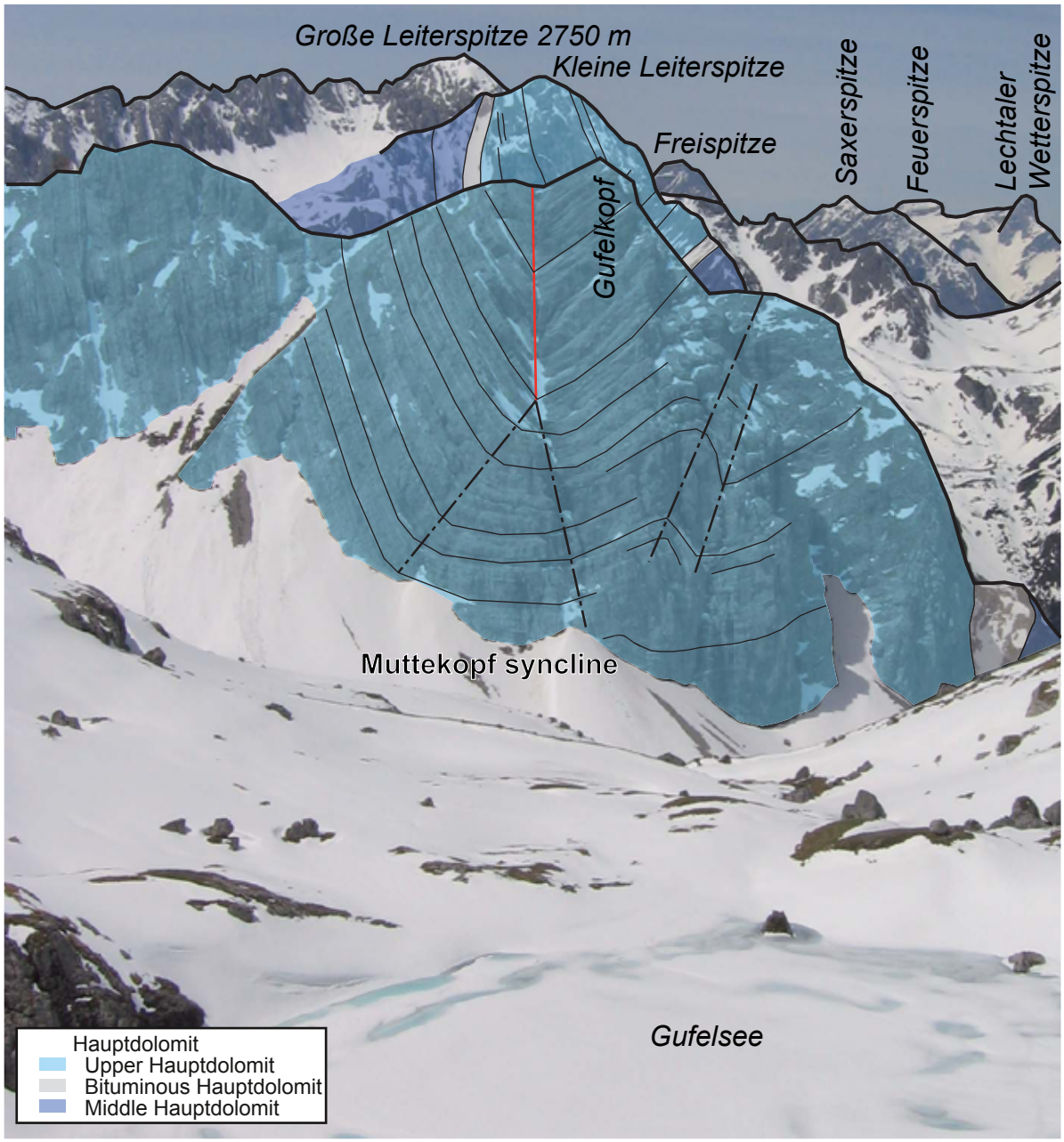

Fig. 22: View to the west at Stop 17. The Muttekopf syncline is seen to continue for 3 km to the Kleine Leiterspitze where it terminates against a tear fault. In the foreground, secondary folds in the nortern limb of the Muttekopf syncline are seen to develop by a progressive increase in amplitude above a minor buckle.

Stop 17, Gufelseejöchl (47°14'32.63"N, 10°34'28.30"E)

We follow the path to the Kogelseespitze and reach the Gufelseejöchl. At this point we stand almost exactly in the core of the Muttekopf syncline, which is exposed 100 m to the south. We have the view of the western continuation of the Muttekopf syncline. In the first ridge to the west with the Gufelkopf summit, the Muttekopf syncline is a box fold that is broken in the core above the branch point of the axial planes (Fig. 22). In the next ridge, with the Kleine Leiterspitze summit, located 3 km behind the Gufelspitze ridge,

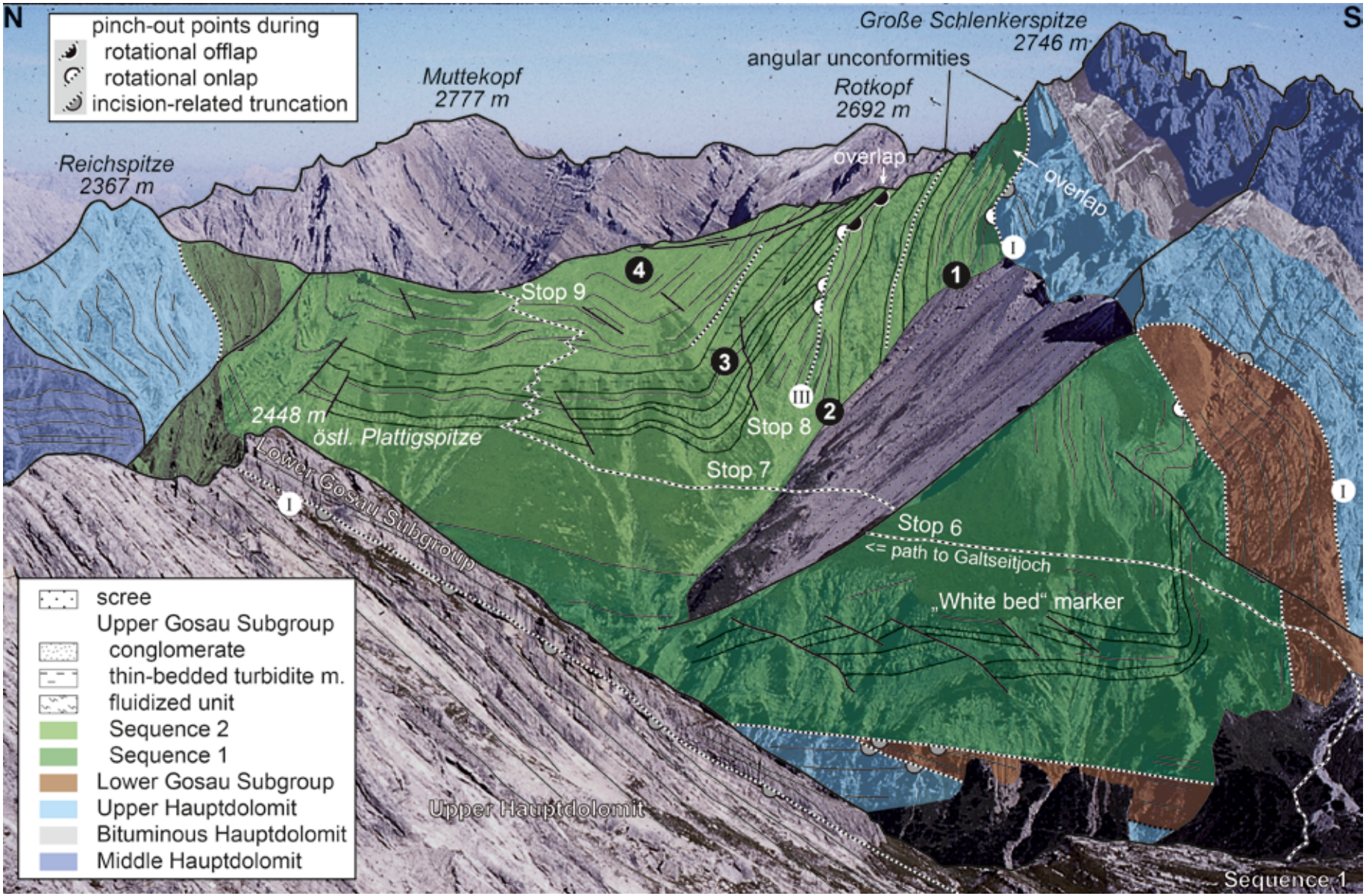

Fig. 23: View to the east at Stop 18, giving an overview of the field trip area (modified from Ortner, 2001). Angular unconformities: I = Schlenkerspitze unconformity, III = Schlenkerkar unconformity. The Parzinn unconformity and related incision is absent in this part of the basin and the base of the "White bed" marker conformable. 1 - 4 denote domains in the steep southern limb of the Muttekopf syncline separated by angular unconformities that were used to separate groups of bedding orientations in diagrams (h) and (i) of Figure 12. Note truncation of Hauptdolomit in the foreground below Plattigspitze, that gives evidence of growth of the Bockkar anticline during deposition of the Gosau Group.

the syncline is still visible, but it ends against a tear fault between Kleine and Große Leiterspitze.

From Gufelseejöchl, we follow the ridge to the north to the Kogelseespitze summit. Along this ridge the column section Kogelseespitze of Figure 8 was measured (Ortner, 1990). During more recent efforts to measure the section it turned out that part of the section has three repetitions of a coarse-grained interval (Amerman, 2009).

Stop 18, Kogelseespitze (47°14'32.63"N, 10°34'28.30"E)

The Kogelseespitze summit is exactly at the contact between the Upper Hauptdolomit and Gosau Group. The view gives a fantastic overview of the basin between the Muttekopf - Rotkopf ridge and the Kogelseepitze - Parzinn ridge, and especially of the Reichspitze - Schlenkerspitze ridge (Fig. 23).

When comparing the eastern, Galtseitjoch, and western, Plattigspitze - Kogelseepitze area, one of the most striking differences are dramatically different sedimentary thicknesses. While Sequence 1 has a thickness of 170 m in the northern limb of the Muttekopf syncline north of Schlenkerkar (Amerman, 2009), it is only 120 m in the Kogelseespitze section, and a few 10s of meters in the Plattigspitze area. Where the sedimentary column is thin, growth structures are more prominent, e.g., near Plattigspitze (Fig. 20). This is especially pronounced, as the wavelength and amplitude of folding increases to the west, while the sedimentary thicknesses decrease.

4 Interpretation and Outlook

In summary, two fundamentally different types of synorogenic sediments have been visited: The upper-footwall deposits of the Lech Fm. below the Inntal thrust sheet, and the thrust-sheet top deposits of the Gosau Group on top of the Inntal thrust sheet. The main differences are (1) the unconformable contact of the thrust-sheet top deposits to pre-orogenic rocks as compared to a conformable transition into upper-footwall deposits, (2) the coarse-grained character of the first versus the generally fine-grained nature, with isolated olistoliths, of the latter, and (3) the presence of clear growth structures in the first and their absence in the latter. Generally, the Gosau Group and part of the Branderfleck Fm. of the Northern Calcareous Alps have the character of thrust-sheet top deposits, and the Lech, Tannheim, Schrambach, Losenstein and Roßfeld Fms. are upper-footwall deposits (Fig. 2).

The joined interpretation of all synorogenic deposits puts some new constraints on the Cretaceous tectonic evolution of the Northern Calcareous Alps. Uplift and subaerial exposure of the Inntal thrust sheet until the Coniacian is contemporaneous with deep marine sedimentation on the Northern Lechtal thrust sheet, that was uplifted and eroded between the Late Albian and Early Cenomanian. In the westernmost part of the Lechtal thrust sheet, sedimentation was continuous from the Triassic into the Turonian. However, all uplifted units subsided to deep marine conditions while shortening was still ongoing. Regional subsidence was overprinted by local, thrust-related uplift. In the most external part of the orogenic wedge uplift is short-lived (see above), while in more internal parts of the wedge the time between the youngest upper-footwall deposits and the oldest thrust-sheet-top deposits increases significantly, i.e., Albian to Cenomanian for the Northern Lechtal thrust sheet, Albian to Turonian for the southeastern Lechtal thrust sheet, Cenomanian to Coniacian in the western Inntal thrust sheet. This is in accordance with the assumption of a growing and subsiding orogenic wedge. Most probably the Northern Calcareous Alps were subject to foreland subsidence, that was intermittently interrupted by local uplift due

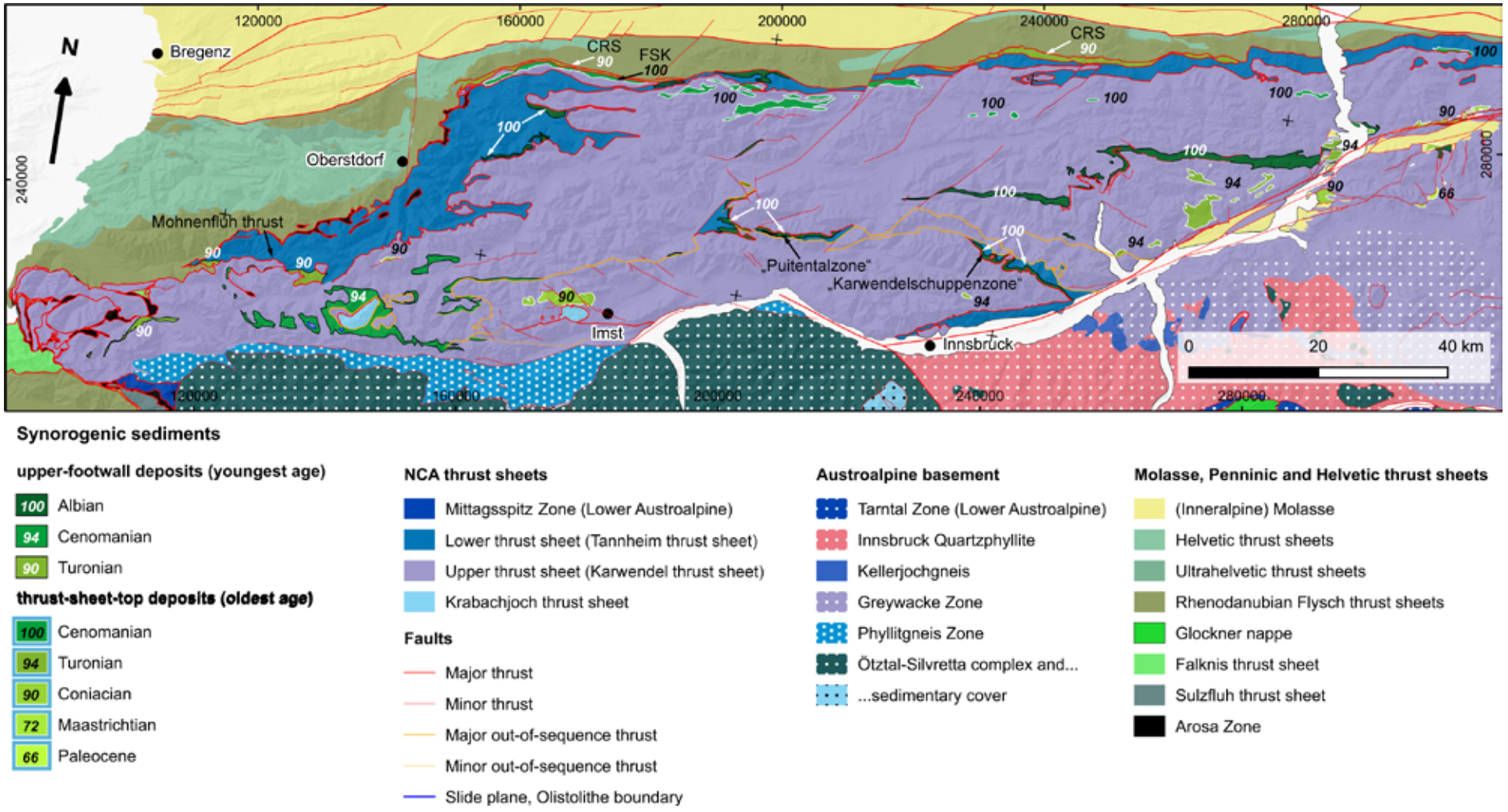

Fig. 24: Tectonic subdivision of the western part of the Northern Calcareous Alps in accordance with the ages and distribution of upper-footwall- and thrust-sheet-top deposits. The nappe structure can be explained by only two large tectonic units, however, the distinction of in-sequence and out-of-sequence thrusts is necessary. Abbreviations: CRS = Cenomanrandschuppe, color denotes upper-footwall deposits reaching into the Turonian. FSK = Falkenstein klippe, an external part of the Lechtal thrust sheet. Graticule: MGI/Austria GK M28 (EPSG: 31257).

to stacking of thrust sheets and/or folding-related thickening. For this reason subsidence diagrams for the Gosau Group (Wagreich, 1991) are comparable to those for e.g. the Cenozoic Alpine peripheral foreland basin (Genser et al., 2007; Zweigel et al., 1998) and its Paleogene wedge top (Ortner & Sachsenhofer, 1996), with increasing subsidence through time.

If the ramp-flat model as outlined in the chapter 2 "Geological setting" was entirely true, one would expect that thrust planes are always accompanied by upper footwall-deposits. The geologic map (Fig. 3, 24) shows that this is not the case. In fact, upper footwall-deposits are restricted to synclines in the footwall that do not affect the thrust, both below the in-sequence Lechtal thrust and the out-of-sequence Inntal thrust. Therefore the ramp-flat model is probably not appropriate. We speculate that only a model of thrust propagation involving significant footwall deformation can describe these thrusts correctly (Ortner & Kilian, 2013, 2014).

The distribution of thrust-sheet-top deposits and upper-footwall deposits can be used to outline the Cretaceous thrust sheets of the Northern Calcareous Alps. The Inntal thrust sheet in Figure 3 is seen to rest on Cenomanian upper-footwall deposits west of Imst, while east of Imst, the youngest upper-footwall deposits are of Albian age. Therefore, the contact between the Inntal- and Lechtal thrust sheets in the Wetterstein mountains and the Karwendel mountains E of Imst should be parallelized with the contact between the Lechtal and Allgäu thrust sheets at the northern margin of the Northern Calcareous Alps, where upper-footwall deposits of the same age are found. Both in the Karwendel mountains and in in the Wetterstein mountains, the contact between upper-footwall sediments and the overlying thrust sheet is offset by younger out-of-sequence thrusts (Kilian, 2013), which were used by Tollmann (1976) to delimit his Inntal thrust sheet. These out-of-sequence thrust do not display the diagnostic old-over-young relationship. Only in the continuation to the west, where offset across these out-of-sequence thrusts increases, the Inntal thrust sheet is emplaced onto Cenomanian upper-footwall deposits.

Further research may result in a revised nappe subdivision in the western part of the Northern Calcareous Alps (Fig. 24), which is in accordance with the distribution and ages of Cretaceous upper-footwall- and thrust-sheet-top deposits (see also Ortner & Kilian, 2013). The former Inntal and Lechtal thrust sheets are merged to an Upper thrust sheet (Karwendel thrust sheet), so that the zone of slices in the Karwendel ("Karwendelschuppenzone"; Heissel, 1978) and the Gaistal ("Puitentalzone"; Tollmann, 1970) are a half window and a window, respectively. These were exhumed during Cenomanian out-of-sequence thrusting. The absence of clear thrust-related structures with klippen or half-klippen on top of upper-footwall deposits documents the absence of a major thrust between the former Lechtal- and Tirolic units. Consequently, also the Tirolic unit is part of this Upper thrust sheet. A Lower thrust sheet (Tannheim thrust sheet) includes the former Allgäu thrust sheet and the slices of the "Puitentalzone" and the "Karwendelschuppenzone" (Fig. 24). The Albian Lechtal thrust ends in the Arlberg region, and is replaced to the west by the Coniacian to Santonian Mohnenfluh thrust (Ortner & Kilian, 2013). However, during later (?Paleogene) reactivation, the two thrusts merged, otherwise the klippen of the Upper thrust sheet (e.g., Karhorn klippe; May & Eisbacher, 1999) could not have been emplaced. To the east, the Albian Lechtal thrust ends somewhere between the Walchensee and the Inn valley. East of the Inn valley both the Lower and the Upper thrust sheet have thrust-sheet-top deposits, and the thrust boundary inbetween must postdate both and be of Paleogene age (Fig. 24).

Acknowledgements

The laserscanning images in the background of Figures 5, 10 and 11 appear courtesy of the Tyrolean government (data source: Land Tirol - data.tirol.gv.at), which is greatly acknowledged. The maps of Figures 3, 5, 10, 11, 14, 24 have been created with the Quantum GIS freeware. I thank the Quantum GIS team for their useful software. I acknowledge Midland Valley for providing their Move software in the frame of their academic software initiative. Move was used to construct the cross sections of Figure 9. The text benefitted from critical comments by M. Strasser (Innsbruck) and A. Gruber (Wien).

5 References

Amerman, R. (2009): Deepwater mass-transport deposits: structure, stratigraphy, and implications for basin evolution.– 238 S., unpubl. PhD thesis Colorado School of Mines, Golden, USA.

Ampferer, O. (1942): Geologische Formenwelt und Baugeschichte des östlichen Karwendelgebirges.– Denkschriften d. Akad. d. Wiss., 106 (1): 1-95.

Ampferer, O. & Hammer, W. (1911): Geologischer Querschnitt durch die Alpen vom Allgäu zum Gardasee.– Jb. Geol. Reichsanst., 61: 531-710.

Ampferer, O., Reithofer, O. & Hammer, W. (1932): Geologische Karte der Lechtaler Alpen 1:25.000 – Parseierspitzgruppe.– Geologische Bundesanstalt, Wien.

Biehler, D. (1990): Strukturelle Entwicklung der penninisch-ostalpinen Grenzzone am Beispiel der Arosa-Zone im Ost-Rätikon.– Eclogae Geol. Helv., 83: 221-402.

Bischof, M., Garber, C., Mackowitz, J., Postl, M. & Ortner, H. (2010): Jurassische Beckenbildung in den westlichen nördlichen Kalkalpen.– PANGEO 2010, Abstracts, Journal of Alpine Geology, 52: 93-94.

Dietrich, V. J. & Franz, U. (1976): Ophiolithdetritus in den santonen Gosauschichten (Nördliche Kalkalpen).– Geotekt. Forsch., 50: 85 - 109.

Doert, U. & Helmcke, D. (1976): Geologie des Flexenpasses (Vorarlberg, Österreich).– Geologica et Paleontologica, 10: 181-200.

Donofrio, D. A., Brandner, R. & Poleschinski, W. (2003): Conodonten der Seefeld-Formation: ein Beitrag zur Bio- und Lithostratigraphie der Hauptdolomit-Plattform (Obertrias, westliche Nördliche Kalkalpen, Tirol).– Geol.–Paläontol. Mitt. Innsbruck, 26: 91-107.

Eisbacher, G. H. & Brandner, R. (1995): Role of high-angle faults during heteroaxial contraction, Inntal thrust sheet, Northern Calcareous Alps, western Austria.– Geol.–Paläontol. Mitt. Innsbruck, 20: 389 - 406.

Eisbacher, G. H. & Brandner, R. (1996): Superposed fold thrust structures and high angle faults, northwestern Calcareous Alps, Austria.– Eclogae Geol. Helv., 89: 553-571.

Eisbacher, G. H., Linzer, G.–H. & Meier, L. (1990): A depth extrapolated structural transect across the Northern Calcareous Alps of Western Tirol.– Eclogae Geol. Helv., 83 (3): 711-725.

Ekdale, A. A. (1985): Paleoecology of the marine endobenthos.– Paleogeogr. Paleoclimatol. Paleoecol., 50: 63 - 81.

Eynatten, H. v. (1996): Provenanzanalyse kretazischer Siliziklastika aus den nördlichen Kalkalpen: Petrographie, Mineralchemie und Geochronologie des frühalpidisch umgelagerten Detritus.– 145 S., unpublished PhD thesis Univ. Mainz, Mainz.

Flügel, H. & Fenninger, A. (1966): Die Lithogenese der Oberalmer Schichten und der mikritischen Plassenkalke (Tithonium, Nördliche Kalkalpen).– N. Jb. Geol. Paläont., Abh., 123 (3): 249-280.

Ford, M., Williams, E. A., Artoni, A., Verges, J. & Hardy, S. (1997): Progressive evolution of a fault-related fold pair from growth strata geometries, Sant Llorens de Morunys, SE Pyrenees.– J. Struct. Geol., 19: 413-441.

Frank, W. (1987): Evolution of the Austroalpine elements in the Cretaceous.– In: Flügel, H. W. & Faupl, P., Geodynamics of the Eastern Alps, 379 - 406, Deuticke, Wien.

Frisch, W. & Gawlick, H.–J. (2003): The nappe structure of the central Northern Calcareous Alps and its disintegration during Miocene tectonic extrusion – a contribution to understanding the orogenic evolution of the Eastern Alps.– Int. Jour. Earth Sci., 92: 712-727.

Froitzheim, N. & Manatschal, G. (1996): Kinematics of Jurassic rifting, mantle exhumation, and passive-margin formation in the Austroalpine and Penninic nappes (eastern Switzerland).– Geol. Soc. Am. Bull., 108: 1120-1133.

Froitzheim, N., Schmid, S. M. & Frey, M. (1996): Mesozoic paleogeography and the timing of eclogite-facies metamorphism in the Alps: A working hypothesis.– Eclogae Geol. Helv., 89: 81-110.

Garrison, R. E. & Fischer, A. G. (1969): Deep water limestones and radiolarites of the Alpine Jurassic.– In: Friedmann, G. M., Depositional environments in carbonate rocks – a symposium, 20-56, SEPM Spec. Publ. 14, Tulsa.

Gaupp, R., Eynatten, H. v., Ortner, H. & Sanders, D. (1997): From passive to active margin: Cretaceous synorogenic deposition in the Northern Calcareous Alps.– Gaea Heidelbergensis, 4: 53-77.

Gawthorpe, R. & Hardy, S. (2002): Extensional fault-propagation folding and base-level change as controls on growth-strata geometries.– Sediment. Geol., 146: 47-56.

Genser, J., Cloething, S. A. P. L. & Neubauer, F. (2007): Late orogenic rebound and oblique Alpine convergence: New constraints from subsidence analysis of the Austrian Molasse basin.– Glob. Planet. Change, 58: 214-233, doi: 10.1016/j.gloplacha.2007.03.010

Gröger, M., Ortner, H. & Haas, C. (1997): Flysch-Spurenfossilassoziationen in der Höheren Muttekopfgosau (Oberkreide) nordwestlich von Imst.– Geol.–Paläontol. Mitt. Innsbruck, 22: 153 - 158.

Haas, C. (1991): Zur Geologie und Sedimentologie der östlichen Muttekopfgosau.– 117 S., unpubl. Diploma thesis Univ. Innsbruck, Innsbruck.

Hahn, F. F. (1912): Versuch einer Gliederung der austroalpinen Masse westlich der österreichischen Traun.– Verh. Geol. Reichsanst., 1912: 337-344.

Hahn, F. F. (1913): Grundzüge des Baues der nördlichen Kalkalpen zwischen Inn und Enns.– Mitt. Österr. Geol. Ges., 9: 374-500.

Heissel, G. (1978): Karwendel - geologischer Bau und Versuch einer tektonischen Rückformung.– Geol.– Paläontol. Mitt. Innsbruck, 8: 227 - 288.

Huckriede, R. (1958): Die Kreideschiefer bei Kaisers und Holzgau in den Lechtaler Alpen (Apt - unteres Cenoman).– Verh. Geol. Bundesanst., 1958: 71-86.

Jacobshagen, V. (1965): Die Allgäuschichten (Jura-Fleckenmergel) zwischen Wettersteingebirge und Rhein.– Jb. Geol. Bundesanst., 108: 1-114.

Kilian, S. (2013): Bericht 2012 über geologische und strukturgeologische Aufnahmen im Karwendelgebirge auf UTM-Blatt 2223 Innsbruck.– Jb. Geol. Bundesanst., 153: 411-417.

Lahodinsky, R. (1988): Bericht 1983-1987 über geologische Aufnahmen im Rahmen der Suche nach der Kreide - Tertiär - Grenze (Grundlagenforschung).– Jb. Geol. Bundesanst., 131 (3): 485-488.

Lammerer, B. & Weger, M. (1998): Footwall uplift in an orogenic wedge: the Tauern Window in the Eastern Alps of Europe.– Tectonophysics, 285: 213 - 230.

Lansigu, C. & Bouroullec, R. (2004): Staircase normal fault geometry in the Grés d'Annot (SE France).– In: Joseph, P. & Lomas, S. A., Deep water sedimentation in the Alpine basin of SE France, 223-240, Special Publication No. 221, Geological Society, London.

Leiss, O. (1990): Neue Aspekte zur Geodynamik und Beckenbildung als Ergebnis der Beckenanalyse von synorogenen Kreidevorkommen innerhalb der nördlichen Kalkalpen (Österreich).– Geol. Rundsch., 79 (1): 47-84.

Linzer, H.–G., Ratschbacher, L. & Frisch, W. (1995): Transpressional collision structures in the upper crust: the fold thrust belt of the Northern Calcareous Alps.– Tectonophysics, 242: 41-61.

May, T. (1998): Kinematik der Krabach-Klippen und des Kreideschieferbeckens, Tirol, Österreich.– 126 S., Unpubl. PhD thesis Univ. Karlsruhe, Karlsruhe.

May, T. & Eisbacher, G. (1999): Tectonics of the synorogenic "Kreideschiefer basin", northwestern Calcareous Alps, Austria.– Eclogae Geol. Helv., 92: 307-320.

Mazzoli, S., Pierantoni, P. P., Borraccini, F., Paltrinieri, W. & Deiana, G. (2005): Geometry, segmentation pattern and displacement variations along a major Apennine thrust zone, central Italy.– J. Struct. Geol., 27: 1940-1953.

Meier, I., Wohlwend, S. & Weissert, H. (2010): Geoweg Rüfikopf – eine Reise durch die Erdgeschichte.– 43 S., Lech Zürs Tourismus GmbH, Lech.

Moser, M. & Pavlik, W. (2011): Provisorische Geologische Karte von Österreich, Blatt 143 - St. Anton am Arlberg, GeoFAST 1:50.000.– Geologische Bundesanstalt, Wien.

Müller-Jungbluth, W.–U. (1971): Sedimentologische Untersuchungen des Hauptdolomits der östlichen Lechtaler Alpen, Tirol.– In: Mostler, H., Beiträge zur Mikrofazies und Stratigraphie von Tirol und Vorarlberg, Festband des Geol. Inst., 300-Jahr-Feier Univ. Innsbruck, 255-308, Innsbruck.

Neubauer, F., Dallmeyer, R. D., Dunkl, I. & Schirnik, D. (1995): Late Cretaceous exhumation of the metamorphic Gleinalm dome, Eastern Alps: kinematics, cooling history and sedimentary response in a sinistral wrench corridor.– Tectonophysics, 242: 79-98.

Neubauer, F., Genser, J. & Handler, R. (2000): The Eastern Alps: Result of a two stage collision process.– Mitt. Österr. Geol. Ges., 92: 117-134.

Oberhauser, R. (1963): Die Kreide im Ostalpenraum aus mikropaläontologischer Sicht.– Jb. Geol. Bundesanst., 106: 1-88.

Ortner, H. (1990): Zur Geologie und Sedimentologie der westlichen Muttekopfgosau (Lechtaler Alpen, Tirol).– 100 S., unpubl. Diploma thesis Univ. Innsbruck, Innsbruck.

Ortner, H. (1994a): Die Muttekopfgosau (Lechtaler Alpen, Tirol/Österreich): Sedimentologie und Beckenentwicklung.– Geol. Rundsch., 83: 197-211.

Ortner, H. (1994b): Die petrographische Entwicklung der Muttekopfgosau (Lechtaler Alpen, Tirol).– Zentralblatt für Geologie und Paläontologie, Teil I, 1992 (11/12): 1355-1371.

Ortner, H. (2001): Growing folds and sedimentation of the Gosau Group, Muttekopf, Northern Calcareous Alps, Austria.– Int. J. Earth Sci. (Geol. Rundsch.), 90: 727-739.

Ortner, H. (2003a): Cretaceous thrusting in the western part of the Northern Calcareous Alps (Austria) – evidences from synorogenic sedimentation and structural data.– Mitt. Österr. Geol. Ges., 94: 63-77.

Ortner, H. (2003b): Local and far field stress - analysis of brittle deformation in the western part of the Northern Calcareous Alps, Austria.– Geol.–Paläontol. Mitt. Innsbruck, 26: 109-131.

Ortner, H. (2007): Styles of soft-sediment deformation on top of a growing fold system in the Gosau Group at Muttekopf, Northern Calcareous Alps, Austria: Slumping versus tectonic deformation.– Sediment. Geol., 196: 99-118.

Ortner, H. (2015): Soft-sediment mullions.– Geophysical Research Abstracts, 17: EGU2015-3891.

Ortner, H. & Gaupp, R. (2007): Synorogenic sediments of the western Northern Calcareous Alps.– Geo.Alp, 4: 133-148.

Ortner, H. & Kilian, S. (2013): In-sequence and out-of-sequence thrusts: nappe structure of the western Northern Calcareous Alps revisited.– Berichte der Geologischen Bundesanstalt, 99 (11th Alpine Workshop, Schladming, Abstract Volume): 72.

Ortner, H. & Kilian, S. (2014): In-sequence and out-of-sequence thrusts: nappe structure of the western Northern Calcareous Alps revisited.– Berichte des Institutes für Erdwissenschaften, Karl-Franzens-Universität Graz, Beitragskurzfassungen PANGEO 2014, 20 (1): 158.

Ortner, H., Kositz, A., Willingshofer, E. & Sokoutis, D. (2015): Geometry of growth strata in a transpressive fold belt in field and analogue model: Gosau Group at Muttekopf, Northern Calcareous Alps, Austria.– Basin Res.: 1-21, doi: 10.1111/bre.12129

Ortner, H. & Sachsenhofer, R. (1996): Evolution of the lower Inntal Tertiary and constraints on the development of the source area.– In: Wessely, G. & Liebl, W., Oil and Gas in Alpidic thrust belts and basins of Central and Eastern Europe, 237 -247, EAEG Spec. Publ. No. 5, EAEG, London.

Peresson, H. & Decker, K. (1997): The Tertiary dynamics of the northern Eastern Alps (Austria): changing palaeostresses in a collisional plate boundary.– Tectonophysics, 272: 125-157.

Petschik, R. (1989): Zur Wärmegeschichte im Kalkalpin Bayerns und Nordtirols (Inkohlung und Illit - Kristallinität).– Frankfurter geowiss. Arb., Serie C, Mineralogie, 10: 259 S.

Pickering, K. T., Stow, D. A. V., Watson, M. P. & Hiscott, R. N. (1986): Deep water facies, processes and models: a review and classification scheme for modern and ancient sediments.– Earth Science Reviews, 23: 75-174.

Pochat, S. & van den Driessche, J. (2007): Impact of synsedimentary metre-scale normal fault scarps on sediment gravity flow dynamics: An example from the Grès d'Annot Formation, SE France.– Sediment. Geol., 202: 796-820.

Puigdefabegras, C., Munoz, J. A. & Verges, J. (1992): Thrusting and foreland basin evolution in the Southern Pyrenees.– In: McClay, K., Thrust Tectonics, 247-254, Chapman & Hall, London.

Ramsay, J. G. (1960): The deformation of early linear structures in areas of repeated folding.– J. Geol., 68 (1): 75-93.

Ramsay, J. G. & Huber, M. I. (1987): The Techniques of Modern Structural Geology, Volume 2: Folds and Fractures.– 700 S., Academic Press, London.

Riba, O. (1976): Syntectonic unconformities of the Alto Cardener, Spanish Pyrenees: A genetic interpretation.– Sediment. Geol., 15: 213-233.

Richthofen, F. F. v. (1859): Die Kalkalpen von Vorarlberg und Nord-Tirol: Erste Abtheilung.– Jb. k.k. Geol. Reichsanst., 10: 72-137.

Rothmund, S. (2015): Geologie des Vorarlberger Flysch im Walgau (Vorarlberg, Österreich): Relevanz fuer baugeologische Maßnahmen.– 185 S., unpubl. Master-Thesis Univ. Innsbruck, Innsbruck.

Schmid, S. M., Fügenschuh, B., Kissling, E. & Schuster, R. (2004): Tectonic map and overall architecture of the Alpine orogen.– Eclogae Geol. Helv., 97: 93-117.

Schöpfer, M. P. J., Childs, C. & Walsh, J. J. (2006): Localisation of normal faults in multilayer sequences.– J. Struct. Geol., 28 (5): 816-833.

Sinclair, H. D. & Tomasso, M. (2002): Depositional evolution of confined turbidite basins.– Journal of Sedimentary Research, 72: 451-456.

Spengler, E. (1953): Versuch einer Rekonstruktion des Ablagerungsraumes der nördlichen Kalkalpen (1. Teil, Westabschnitt).– Jb. Geol. Bundesanst., 96: 1-64.

Stüwe, K. & Schuster, R. (2010): Initiation of subduction in the Alps: Continent or ocean?- Geology, 38: 175-178.

Tollmann, A. (1970): Tektonische Karte der Nördlichen Kalkalpen: 3. Teil: Der Westabschnitt.– Mitt. Österr. Geol. Ges., 62 (1969): 78-170.

Tollmann, A. (1976): Der Bau der Nördlichen Kalkalpen.– 449 S., Monographie der Nördlichen Kalkalpen, Teil III, Deuticke, Wien.

Wagreich, M. (1991): Subsidenzanalyse an kalkalpinen Oberkreideserien der Gosaugruppe (Österreich).– Zbl. Geol. Paläontol. Teil I, 1990 (11): 1645-1657.

Wagreich, M. (2001): A 400-km-long piggyback basin (Upper Aptian-Lower Cenomanian) in the Eastern Alps.– Terra Nova, 13: 401-406.

Wagreich, M. & Faupl, P. (1994): Paleogeography and geodynamic evolution of the Gosau Group of the Northern Calcareous Alps (Late Cretaceous, Eastern Alps, Austria).– Paleogeogr. Paleoclimatol. Paleoecol., 110: 235-254.

Walker, R. G. (1975): Generalized facies models for resedimented conglomerates of the turbidite association.– Geol. Soc. Am. Bull., 86: 737-748.

Wallbrecher, E. (1986): Tektonische und Gefügeanalytische Arbeitsweisen. Graphische, Rechnerische und Statistische Verfahren.– 244 S., Enke, Stuttgart.

Wentworth, C. K. (1922): A scale of grade and class terms for clastic sediments.– Jour. Geol., 30: 377-392.

Wopfner, H. (1954): Neue Beiträge zur Geologie der Gosauschichten des Muttekopfgebietes.– N. Jb. Geol. Paläont., Abh., 100: 11-82.

Zweigel, J., Aigner, T. & Luterbacher, H. (1998): Eustatic versus tectonic controls an Alpine foreland basin fill: sequence stratigraphy and subsidence analysis in the SE German Molasse.– In: Mascle, A., Cenozoic foreland basins of western Europe, 299-323, Special Publication No. 134, Geological Society, London.